Circulation Research

ORIGINAL RESEARCH

Increased Intermembrane Space [Ca^{2+}] Drives Mitochondrial Structural Damage in CPVT

Shanna Hamilton, Radmila Terentyeva, Roland Veress, Fruzsina Perger, Zuzana Nichtova, Mark Bannister, Jinxi Wang, Sage Quiggle, Rachel Battershell, Matthew W. Gorr, Sandor Györke, Bum-Rak Choi, Christopher H. George, Andriy E. Belevych, György Csordás, Dmitry Terentyev

BACKGROUND: Mitochondrial dysfunction caused by abnormally high RyR2 (ryanodine receptor) activity is a common finding in cardiovascular diseases. Mechanisms linking RyR2 gain of function with mitochondrial remodeling remain elusive. We hypothesized that RyR2 hyperactivity in cardiac disease increases [Ca^{2+}] in the mitochondrial intermembrane space (IMS) and activates the Ca^{2+}-sensitive protease calpain, driving remodeling of mitochondrial cristae architecture through cleavage of structural protein OPA1 (optic atrophy protein 1).

METHODS: We generated a highly arrhythmogenic rat model of catecholaminergic polymorphic ventricular tachycardia, induced by RyR2 gain-of-function mutation S2236L(Ser2336Leu)$^{(+/-)}$. We created a new biosensor to measure IMS-[Ca^{2+}] in adult cardiomyocytes with intact Ca^{2+} cycling. We used ex vivo whole heart optical mapping, confocal and electron microscopy, as well as in vivo/in vitro gene editing techniques to test the effects of calpain in the IMS.

RESULTS: We found altered mitochondrial cristae structure, increased IMS-[Ca^{2+}], reduced OPA1 expression, and augmented mito-reactive oxygen species emission in catecholaminergic polymorphic ventricular tachycardia myocytes. We show that calpain-mediated OPA1 cleavage led to disrupted cristae organization and, thereby, decreased electron transport chain supercomplex assembly, resulting in accelerated reactive oxygen species production. Genetic inhibition of calpain activity in IMS reversed mitochondria structural defects in catecholaminergic polymorphic ventricular tachycardia myocytes and reduced arrhythmic burden in ex vivo optically mapped hearts.

CONCLUSIONS: Our data suggest that RyR2 hyperactivity contributes to mitochondrial structural damage by promoting an increase in IMS-[Ca^{2+}], sufficient to activate IMS-residing calpain. Calpain activation leads to proteolysis of OPA1 and cristae widening, thereby decreasing assembly of electron transport chain components into supercomplexes. Consequently, excessive mito-reactive oxygen species release critically contributes to RyR2 hyperactivation and ventricular tachyarrhythmia. Our new findings suggest that targeting IMS calpain may be beneficial in patients at risk for sudden cardiac death.

GRAPHIC ABSTRACT: A graphic abstract is available for this article.

Key Words: calcium ■ cardiovascular diseases ■ heart failure ■ mitochondrial proteins ■ ryanodine receptor calcium release channel ■ sarcoplasmic reticulum

Editorial, see p 1404

Impaired mitochondrial function and aberrant intracellular calcium (Ca^{2+}) cycling are common findings in various cardiovascular diseases (CVDs) such as heart failure (HF), diabetic cardiomyopathy, and age-related cardiac dysfunction.[1] Disease-associated defects in mitochondrial function lead to excessive production of reactive oxygen species (ROS), which disturb numerous signaling pathways and systems in ventricular myocytes

Correspondence to: Shanna Hamilton, PhD, 1656 E Mabel St, Medical Research Building Room 319, Department of Cellular and Molecular Medicine, University of Arizona, Tucson, AZ, 85721, Email shannahamilton@arizona.edu; or Dmitry Terentyev, PhD, 473 W 12th Ave, Dorothy M. Davis Heart and Lung Research Institute Room 405B, Department of Physiology and Cell Biology, The Ohio State University, Columbus, OH, 43210 Email dmitry.terentyev@osumc.edu

Supplemental Material is available at https://www.ahajournals.org/doi/suppl/10.1161/CIRCRESAHA.125.326841.

For Sources of Funding and Disclosures, see page 1400.

Novelty and Significance

What Is Known?

- RyR2 (ryanodine receptor) hyperactivity and mitochondrial structural damage are common findings in cardiovascular diseases.
- Excessive reactive oxygen species generation by defective mitochondria leads to RyR2 oxidation, promoting RyR2 hyperactivity, contributing to arrhythmogenesis.
- Hyperactive RyR2s can disrupt mitochondrial function by contributing to cytosolic Ca^{2+} and, thereby, Na^{+} overload. Consequent increase in activity of mitochondrial $Na^{+}/Ca^{2+}/Li^{+}$ exchanger (NCLX) reduces the ability of mitochondria to accumulate $[Ca^{2+}]$ in the mitochondrial matrix.

What New Information Does This Article Contribute?

- For the first time, we measure Ca^{2+} in the intermembrane space of cardiac mitochondria and, contrary to current dogma, show that $[Ca^{2+}]$ significantly accumulates in this space, especially in conditions of RyR2 gain of function.
- We provide a molecular mechanism linking RyR2 hyperactivity with mitochondrial structural remodeling, whereby increased Ca^{2+} in the intermembrane space activates calpain-mediated cleavage of mitochondrial structural protein OPA1 (optic atrophy protein 1).
- We demonstrate that calpain-mediated cleavage of OPA1 leads to cristae widening and loss of electron transport chain supercomplexes, leading to emission of damaging reactive oxygen species that further increase RyR2 activity.
- Our data demonstrate the protective effects of inhibiting calpain in the mitochondrial intermembrane space, attenuating Ca^{2+} mishandling at the cellular level and preventing Ca^{2+}-dependent arrhythmia at the organ level.

Increased RyR2 activity due to gain-of-function mutations, posttranslational modifications, or both, leads to a proarrhythmic increase in cytosolic $[Ca^{2+}]$ during diastole, promoting Na^{+} overload in myocytes from diseased hearts. Increased cytosolic $[Na^{+}]$ increases the activity of NCLX, interfering with the ability of mitochondria to retain Ca^{2+} in the matrix. Using a mitochondrial intermembrane space–targeted Ca^{2+} biosensor, we found that Ca^{2+} in this compartment does not precisely follow cytosolic Ca^{2+} dynamics and, instead, accumulates during rapid pacing, significantly exceeding cytosolic $[Ca^{2+}]$ during diastole. Both genetic and pharmacological RyR2 activity enhancements reduced Ca^{2+} retention in mitochondrial matrix, leading to a reciprocal increase in intermembrane space-$[Ca^{2+}]$ to the levels sufficient for activation of intermembrane space–residing Ca^{2+}–dependent protease μ-calpain. Activation of calpain evoked proteolysis of structural protein OPA1, resulting in widening of mitochondrial cristae. Subsequent decrease in the ability of cristae-residing components of the electron transport chain to form supercomplexes resulted in acceleration of mitoreactive oxygen species production, oxidizing RyR2, exacerbating proarrhythmic hyperactivation of the channel. Given the prevalence of RyR2 hyperactivity and mitochondrial dysfunction, this mechanism likely contributes to Ca^{2+} mishandling in a broad spectrum of cardiovascular pathologies. Attenuating intracellular Ca^{2+} mishandling in diseased hearts by targeting intermembrane space calpain may be beneficial in patients at risk for sudden cardiac death.

Nonstandard Abbreviations and Acronyms

AAV	adeno-associated virus
AIF	apoptosis-inducing factor
CAST	calpastatin
CPVT	catecholaminergic polymorphic ventricular tachycardia
CVD	cardiovascular disease
ETC	electron transport chain
HF	heart failure
IMM	inner mitochondrial membrane
IMS	intermembrane space
JPH2	junctophilin-2
MCU	mitochondrial Ca2+ uniporter
MICU	mitochondrial calcium uptake protein
NCLX	mitochondrial $Na^{+}/Ca^{2+}/Li^{+}$ exchanger
OMM	outer mitochondrial membrane
OPA1	optic atrophy protein 1
ROS	reactive oxygen species
RyR2	ryanodine receptor
shRNA	short hairpin RNA
SR	sarcoplasmic reticulum
TG	thapsigargin
VDAC	voltage-dependent anion channel
VM	ventricular myocyte
VT	ventricular tachycardia

(VMs).[2,3] It is well established that mitochondrial ROS increases the activity of the sarcoplasmic reticulum (SR) Ca^{2+} release channel, the RyR2 (ryanodine receptor), thereby driving spontaneous SR Ca^{2+} release that impairs contractile function and promotes deadly arrhythmias.[1,3–5] In turn, abnormally high RyR2 activity may contribute to mitochondrial dysfunction and, importantly, structural damage of the organelle. This is especially obvious in the case of the highly malignant inherited arrhythmia syndrome, catecholaminergic polymorphic ventricular tachycardia (CPVT),[4,6–8] an arrhythmia most commonly linked to gain-of-function mutations in RyR2.[9] Although of growing interest, the exact mechanisms underlying Ca^{2+}-dependent damage of cardiac mitochondria remain undefined.

During ischemia-reperfusion, intracellular Ca^{2+} overload evokes massive Ca^{2+} influx into the mitochondrial matrix via MCU (mitochondrial Ca^{2+} uniporter), leading to mitochondria permeability transition and activation of cell death pathways.[10,11] However, in conditions less catastrophic than ischemia-reperfusion injury such as HF or cardiac hypertrophy, matrix [Ca^{2+}] was shown to be reduced, suggesting that other mechanisms are involved.[12–16] Furthermore, key proteins that maintain mitochondria structure such as prohibitins and OPA1 (optic atrophy protein 1) are located outside of the matrix, between outer and inner mitochondria membranes (OMM and IMM, respectively).[17,18] Although there is substantial data implicating changes in matrix [Ca^{2+}] in cardiac pathophysiology, there is no information on [Ca^{2+}] in the mitochondrial intermembrane space (IMS). This compartment is generally thought to have [Ca^{2+}] equal to that of the cytosol, as the OMM is considered permeable for Ca^{2+}.[19] However, to our knowledge, this has not been experimentally confirmed as IMS [Ca^{2+}] was not measured directly in cardiac VMs due to the lack of appropriate molecular tools.

Previous studies revealed that μ-calpain, an important Ca^{2+}-dependent cysteine protease that senses [Ca^{2+}] in the micromolar range, is localized in the IMS.[20,21] It is plausible that under conditions accompanied by increased RyR2 activity, IMS-[Ca^{2+}] may reach these levels, sufficient to activate μ-calpain in this compartment. Importantly, recent works from several laboratories suggest that calpain inhibition can improve mitochondrial function in diseased or aging hearts.[22–25] However, the mechanisms of calpain-dependent mitochondrial injury in CVD remain unknown. Intriguingly, expression levels of IMS-located mitochondrial structural protein OPA1 are decreased in HF.[26] Whether Ca^{2+}-dependent calpain activity in the IMS can lead to proteolysis of mitochondrial proteins and, thus, drive changes in mitochondrial structure is yet to be explored.

To test the hypothesis that RyR2 hyperactivity evokes changes in IMS-[Ca^{2+}], we created a unique gain-of-function RyR2 rat model of CPVT and a novel, targeted genetic Ca^{2+} probe. Using this linear model of disease-associated RyR2 dysfunction, we demonstrate that increased Ca^{2+}-dependent calpain activity in the IMS drives mitochondrial structural remodeling, increasing mito-ROS production, and this contributes to cardiac arrhythmia. Furthermore, we show that gene delivery approaches to reduce IMS calpain activity in CPVT can attenuate mitochondrial structural damage and dysfunction, reducing proarrhythmic disturbances in intracellular Ca^{2+} cycling. These data reveal the previously unappreciated importance of IMS-[Ca^{2+}] in mitochondrial structure, which does not simply follow cytosolic [Ca^{2+}], as well as the strong therapeutic potential of targeting Ca^{2+}-dependent processes in this subcompartment to attenuate Ca^{2+}-dependent arrhythmia in CVD.

METHODS

Data Availability

Data supporting the findings of this study are available from the corresponding authors upon reasonable request. Detailed materials and methods are described in the Supplemental Material. Key research materials are listed in the Major Resources Table in the Supplemental Material. All procedures involving animals were performed following the National Institutes of Health Guide for the Care and Use of Laboratory Animals published by the US National Institutes of Health (National Institutes of Health Publication No. 85-23, revised 2011). Procedures were approved by the Institutional Animal Care and Use Committee of The Ohio State University, The University of Arizona, or Thomas Jefferson University.

Statistical Analysis

Statistical analyses were performed using Origin 2020Pro (OriginLab) and R software. For each experiment, the number of animals (N) and the number of VMs (n) used are indicated. Data are expressed as mean±SD. *P* values are provided with 2 significant digits, and values of $P<0.050$ were considered significant (*). When we used individual isolated VMs from rat hearts, data were analyzed using a 2-level random intercept model to account for multiple cells (data points) from one animal and hierarchical data.[19,27,28] For nonhierarchical data (isolated VMs from one rat heart per animal, for example), the Shapiro-Wilk tests were performed to determine normality of data. More detail is given in the Supplementary Material.

RESULTS

The Novel RyR2-S2236L$^{(+/-)}$ Rat Model of CPVT Exhibits a Strong Arrhythmogenic Phenotype

To directly test whether a disease-associated increase in RyR2 activity modulates IMS-[Ca^{2+}], we created the first rat model of RyR2-associated CPVT. The malignant RyR2-S2236L$^{(+/-)}$ mutation (Figure 1A) was chosen as it induces archetypical CPVT phenotype in humans (RyR2-S2246L$^{(+/-)}$; Figure S1).[29–32]

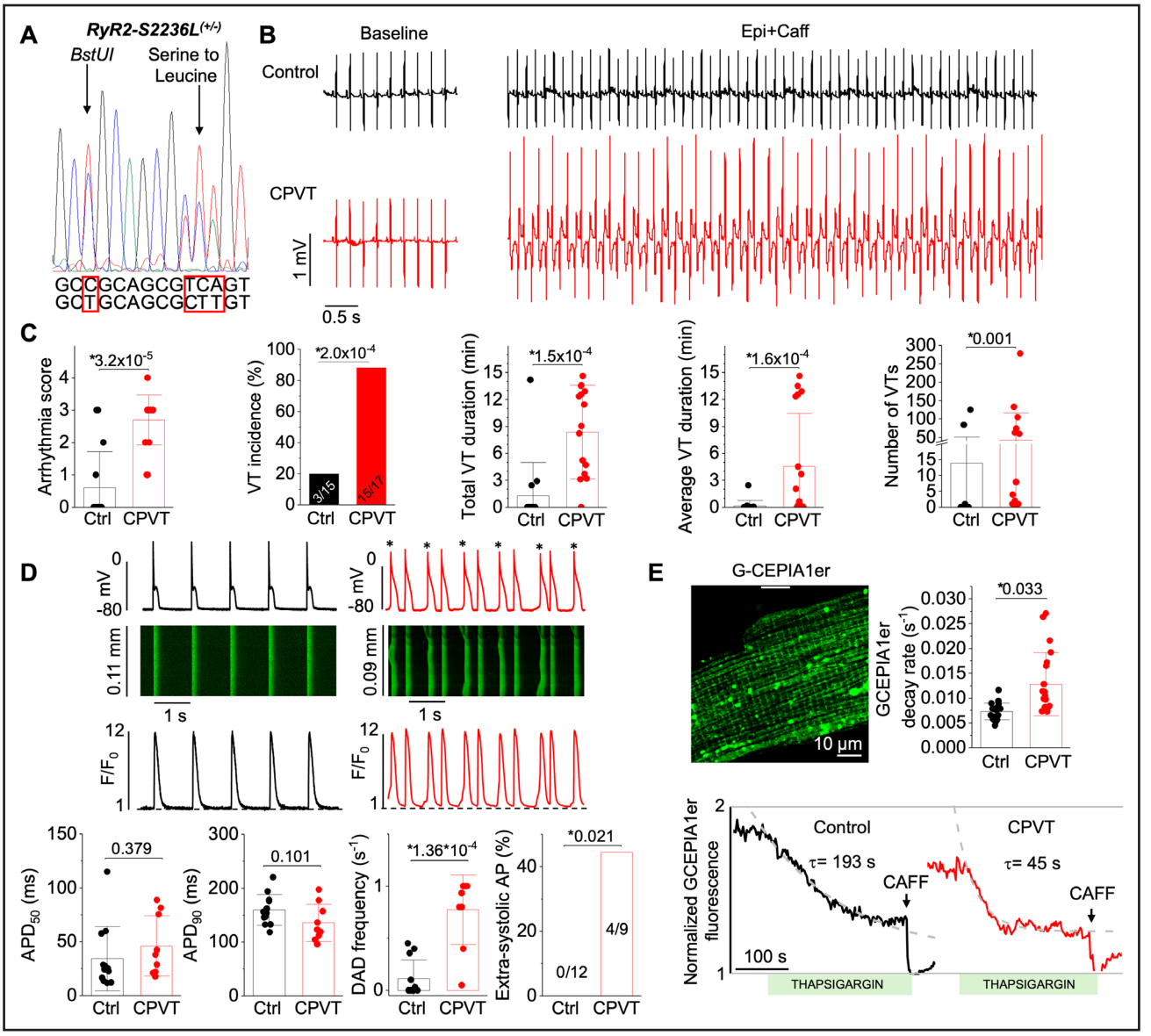

Figure 1. The novel *RyR2-S2236L*$^{(+/-)}$ rat model of catecholaminergic polymorphic ventricular tachycardia (CPVT) exhibits a robust arrhythmogenic phenotype.

A, Chromatogram demonstrating CRISPR/Cas9 (clustered regularly interspaced short palindromic repeats/CRRISPR-associated protein 9)-mediated heterozygous *RyR2-S2236L*$^{(+/-)}$ mutation. **B**, In vivo electrocardiograms of littermate control and CPVT rats, before and after intraperitoneal (IP) injection with epinephrine (1 mg/kg) and caffeine (120 mg/kg) as arrhythmia challenge. **C**, Arrhythmia score based on the most severe arrhythmia was applied: no arrhythmias=0; isolated premature ventricular complex (PVC)=1; nonsustained ventricular tachycardia (VT; <30 s)=2; sustained VT (>30 s)=3; and ventricular fibrillation=4. Ventricular tachycardia was defined as ≥3 consecutive PVCs. *P<0.05, Mann-Whitney U test. VT incidence (%), Fisher exact test. Total VT duration (minutes), Mann-Whitney U test. Average VT duration (minutes), *P<0.05, Mann-Whitney U test. Number of VTs, Mann-Whitney U test. N for in vivo ECG experiments: control (Ctrl): N=15 (7 female, 8 male) rats; CPVT: N=17 (10 female, 7 male) rats. **D**, Simultaneous action potential and intracellular Ca^{2+} recordings under β-adrenergic stimulation with isoproterenol (ISO; 50 nmol/L) and corresponding pooled data for action potential duration $(APD)_{50}$, APD_{90}, frequency of delayed after depolarizations (DADs), and extra-systolic action potentials (APs). Data are presented as mean±SD, 2-level random intercept model. Control: n=7 cells, N=4 (3 female, 1 male) rats; CPVT: n=6 cells, N=4 (1 female, 3 male) rats. **E**, The image shows the ventricular myocyte expressing sarcoplasmic reticulum (SR) Ca^{2+} probe G-CEPIA1er. Representative G-CEPIA1er fluorescence recorded in control (Ctrl, black) and CPVT (red) ventricular myocytes. Myocytes were treated with ISO (50 nmol/L) and paced for 5 minutes at 2 Hz prior to application of thapsigargin (20 µmol/L, 5 minutes) to inhibit SERCA2a (cardiac sarcoplasmic reticulum calcium ATPase) activity. Caffeine (CAFF; 10 mmol/L) was used to fully empty the SR. The signal was normalized to the minimum fluorescence obtained after caffeine application. Two-level random intercept model. Control: n=19 cells, N=6 (3 female, 3 male) rats; CPVT: n=20 cells, N=5 (3 male, 2 female) rats.

Patients with CPVT under basal conditions do not exhibit profound changes in cardiac function and gross structural remodeling of the heart.[9,33,34] In line with this, echocardiography recordings did not reveal gross structural remodeling of the heart in CPVT rats, given preserved left ventricle posterior wall size and calculated left

ventricle mass compared with littermate controls (Table S2). Ejection fraction, fractional shortening, and E/E' were unchanged, indicating no alterations in systolic and diastolic function.

To confirm the CPVT phenotype in vivo, we performed an ECG with arrhythmia challenge, a widely used protocol to elicit arrhythmias in animal models of CPVT (Figure 1B and 1C; Figure S2). Injection of epinephrine (1.5 mg/kg) and caffeine (120 mg/kg) induced significantly higher incidences of bigeminy, bidirectional ventricular tachycardia (VT), and ventricular fibrillation in vivo in heterozygous CPVT animals, as indicated by a higher arrhythmia score ($*P=3.2\times10^{-5}$), and an overall increased incidence of VT ($*P=2.0\times10^{-4}$).

Simultaneous whole cell patch clamp and Ca^{2+} imaging with fluorescent Ca^{2+} indicator Rhod-2 demonstrated that under β-adrenergic stimulation with isoproterenol (50 nmol/L), CPVT VMs exhibit severe Ca^{2+} mishandling compared with controls. There is no obvious Ca^{2+} mishandling in CPVT VMs under baseline conditions (Figure S3). Periodically paced CPVT VMs in the presence of isoproterenol have a high propensity to generate spontaneous Ca^{2+} release during diastole, which causes arrhythmogenic delayed afterdepolarizations, a hallmark of CPVT (Figure 1D; Figure S4). Importantly, delayed afterdepolarizations occurred without significant electrophysiological remodeling (Figure S5; Figure 1D), implying that these are Ca^{2+}-driven.

To confirm that RyR2-S2236L$^{(+/-)}$ VMs exhibit increased SR Ca^{2+} leak, SR Ca^{2+} biosensor G-CEPIA1er was expressed using an adenovirus vector construct.[4,35] After 36 to 48 hours in culture, isoproterenol-treated VMs were exposed to thapsigargin, an SR-Ca^{2+} ATPase inhibitor (TG, 20 µmol/L), to unmask RyR2-mediated SR Ca^{2+} leak. Data presented in Figure 1E demonstrate a 2-fold increase in leak rate in CPVT VMs versus controls ($*P=0.033$).

Hyperactivity of RyR2 in CPVT Increases Mitochondrial ROS and Disrupts Mitochondrial [Ca^{2+}] Handling

It has been demonstrated previously that increasing RyR2 activity leads to spontaneous SR Ca^{2+} release and evokes increased mitochondrial ROS emission.[4] This exacerbates RyR2 dysfunction in a vicious feedback cycle. Indeed, in this study, adenoviral genetic probe MLS-HyPer7[13,36] confirmed significantly increased mitochondrial ROS in cultured CPVT VMs versus controls treated with isoproterenol (Figure 2A, $*P=1.0\times10^{-4}$). Representative fluorescence recordings demonstrating changes in mitochondrial ROS before and after isoproterenol are found in Figure S6. Importantly, the increase in mitochondrial ROS in CPVT VMs was in parallel with increased RyR2 oxidation (Figure 2B, $*P=0.008$). Using adenoviral genetic probe mtRCamp1h,[12,37] our data reveal reduced [Ca^{2+}] in the mitochondrial matrix of periodically paced CPVT VMs challenged with isoproterenol (50 nmol/L) compared with controls (Figure 2C, $*P=0.004$; Figure S7, $*P=4.88\times10^{-7}$). These data suggest that increased mitochondrial ROS production occurs in CPVT VMs with increased RyR2 leak, despite reduced mitochondrial matrix [Ca^{2+}]. Of note, Western blot analysis did not reveal changes in expression levels of voltage-dependent anion channel (VDAC) and MCU, the main Ca^{2+} pathways residing in outer and inner mitochondrial membranes, respectively (Figure 2D and 2E). Expression levels of auxiliary proteins of mitochondria Ca^{2+} uptake complex MCUb[38] and MICU (mitochondrial calcium uptake protein) 2[39] were not changed, while MICU1, a negative regulator of MCU,[40] was decreased ($*P=0.004$). Despite this change, Ca^{2+} uptake into the matrix was similar in control and CPVT, as demonstrated by experiments in permeabilized VMs using an identical intracellular solution (Figure S8). Given that matrix Ca^{2+} levels depend on NCLX (mitochondrial $Na^+/Ca^{2+}/Li^+$ exchanger) activity,[41] we measured intracellular [Na^+] using fluorescence indicator ING-2. Field-stimulated CPVT VMs loaded with ING-2 and treated with 50 nmol/L isoproterenol showed a significant increase in intracellular [Na^+] (Figure S9, $*P=0.043$). Stabilization of intracellular Ca^{2+} handling using mitochondrial ROS scavenger MitoTEMPO[4] (5 µmol/L, 20 minutes pre-incubation) reversed cytosolic Na^+ overload and restored matrix Ca^{2+} accumulation in CPVT VMs (Figure S10).

Mitochondrial IMS [Ca^{2+}] Is Increased in Conditions of RyR2 Hyperactivity

We reasoned that increased diastolic [Ca^{2+}] in the cytosol and the reduced ability of the mitochondria to accumulate Ca^{2+} in the matrix could lead to an increase in [Ca^{2+}] in mitochondrial IMS. Given that the current dogma is that the IMS is permissive to Ca^{2+}, we directly measured Ca^{2+} in this compartment with a genetic biosensor. We adapted the cytosolic genetic Ca^{2+} probe GECO1.2[42] (Kd [dissociation constant] of 1.15 µmol/L for Ca^{2+}) by adding the first 140 amino acids of the MCU complex protein MICU1 to the N-terminal of the coding sequence[43] (Figure 3A). Adenovirus was generated for the expression of the probe in cultured rat VMs. Rings of green fluorescent protein were evident in Ad-IMS-GECO1.2–infected VMs after 36 hours, suggestive of correct probe targeting between the OMM and IMM.

To verify correct targeting to the IMS, we added an APEX2 (ascorbate peroxidase 2) tag[44] to the C-terminal of the probe and generated adeno-associated virus (AAV) with cardiac specificity. Rats were tail vein injected with AAV9-αMHC-IMS-GECO1.2-APEX2 (10^{12} viral particles per rat), and left ventricular tissue slices were assessed 4 weeks later by transmission electron microscopy (Figure 3B). Tissues were treated with the

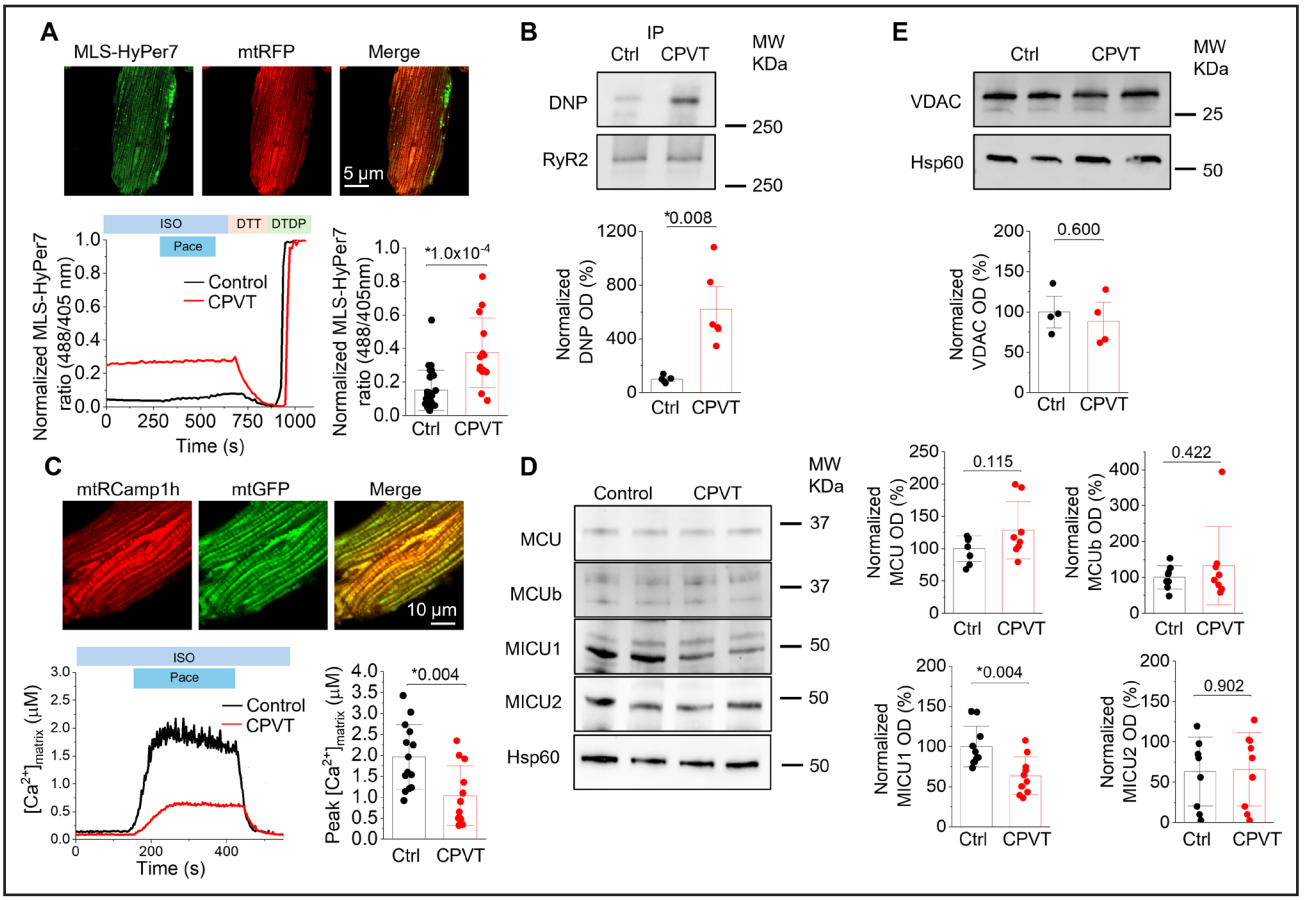

Figure 2. Catecholaminergic polymorphic ventricular tachycardia (CPVT) rat ventricular myocytes have increased mito-reactive oxygen species (ROS) production and reduced matrix [Ca^{2+}].

A, Images show mitochondrial MLS-HyPer7 ROS probe localization in live ventricular myocytes, validated by overlap with mtRFP (mitochondrial RFP [red fluorescent protein]). Representative MLS-HyPer7 fluorescence recorded in control (black) and CPVT (red) ventricular myocytes. Myocytes were treated with isoproterenol (ISO; 50 nmol/L) for 5 minutes before pacing at 2 Hz for 5 minutes. Fluorescence was normalized to minimum (dithiothreitol [DTT]; 5 mmol/L) and maximum (2,2′-dithiodipyridine [DTDP]; 200 µmol/L) fluorescence. Data are presented as mean±SD, *P<0.05, 2-level random intercept model. Control: n=27 cells, N=6 (3 female, 3 male) rats; CPVT: n=14 cells, N=4 (2 female, 2 male) rats. **B**, Representative Western blots for immunoprecipitated RyR2 (ryanodine receptor) from freshly isolated ventricular myocytes and oxidation using anti-DNP antibody. Pooled data for normalized optical density (OD; %) of DNP signal normalized to RyR2, Student t test. Control: N=5 control (3 female, 2 male) rats; CPVT: N=6 (3 female, 3 male) rats. **C**, Images show mitochondrial mtRCamp1h matrix Ca^{2+} probe localization in live ventricular myocytes, validated by overlap with mtGFP (mitochondrial GFP [green fluorescent protein]). Representative mtRCamp1h fluorescence recorded in control (black) and CPVT (red) ventricular myocytes. Myocytes were treated with isoproterenol for 5 minutes before pacing at 2 Hz for 5 minutes. Two-level random intercept model. Control: n=14 cells, N=6 (3 female, 3 male) rats; CPVT: n=12 cells, N=6 (2 female, 4 male) rats. **D**, Representative Western blot of MCU (mitochondrial Ca^{2+} uniporter), MCUb (mitochondrial Ca^{2+} uniporter subunit dominant negative subunit beta), MICU1 (mitochondrial Ca^{2+} uptake protein 1), MICU2 (mitochondrial Ca^{2+} uptake protein 2), Hsp60 (heat shock protein 60), and pooled data for OD normalized to Hsp60. Control: N=8 to 10 (4–5 female, 4–5 male) rats; CPVT: N=8 to 10 (4–5 female, 4–5 male) rats. **E**, Representative Western blot of voltage-dependent anion channel (VDAC) and loading control Hsp60 and pooled data for OD normalized to Hsp60, Mann-Whitney U test. Control: N=4 (2 female, 2 male) rats; CPVT: N=4 (2 female, 2 male) rats.

3,3'-diaminobenzidine. In tissue expressing the probe with the APEX2 tag treated with 3,3'-diaminobenzidine for 10 minutes (left images), IMM is well-defined. Forty minutes of exposure with 3,3'-diaminobenzidine (right images) revealed increased particle density in the IMS. This particle density is caused by a reaction between the APEX2 tag and 3,3'-diaminobenzidine, therefore only occurring where the probe is located. This demonstrates correct localization of the IMS-GECO1.2 Ca^{2+} probe in the IMS of mitochondria.

The general consensus is that IMS-[Ca^{2+}] equals [Ca^{2+}] in the cytosol, given that Ca^{2+} flux via the OMM high-conductance Cl^--channel (VDAC) is fast. To test this, using fast resonant scanning to improve temporal resolution (7 ms per frame), we performed experiments in periodically paced isoproterenol-treated (50 nmol/L) VMs expressing IMS-GECO1.2. As seen in Figure 3C, IMS-[Ca^{2+}] dynamically changes upon VM electrical stimulus, and both basal and peak [Ca^{2+}] in this compartment rise upon increasing stimulation frequency from 0.2 to 2 Hz (basal: *P=2.0×10^{-4}; peak: *P=0.002). Next, we performed experiments where IMS-[Ca^{2+}] was monitored in parallel with recording of cytosolic Ca^{2+} transients using far red fluorescent Ca^{2+} indicator Calbryte 630-AM,

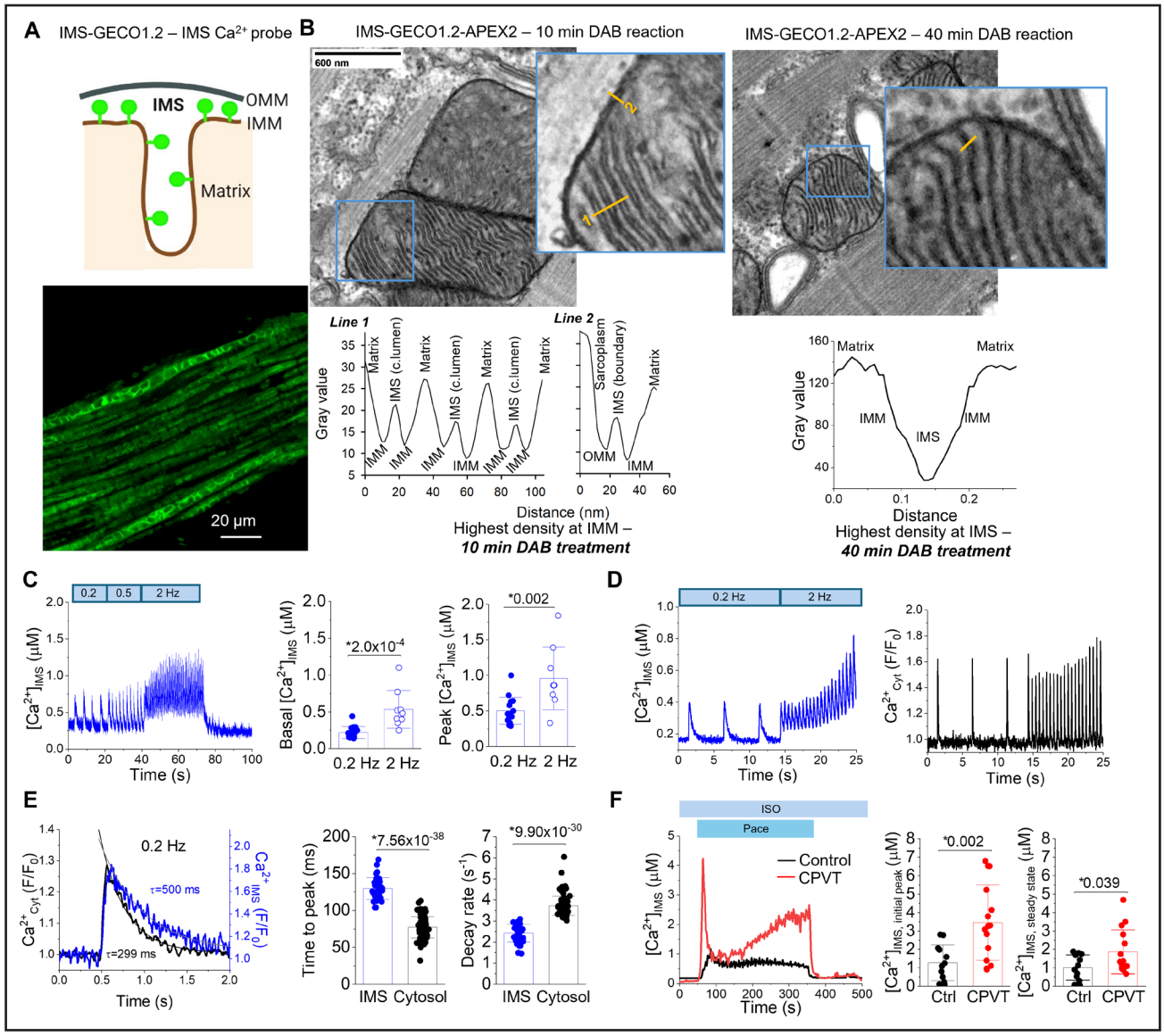

Figure 3. Mitochondrial intermembrane space [Ca^{2+}] does not mirror cytosolic [Ca^{2+}] and is increased in conditions of RyR2 (ryanodine receptor) hyperactivity.

A, **Top**, Schematic of intermembrane space (IMS) Ca^{2+} probe IMS-GECO1.2 location, between the outer and inner mitochondrial membranes (OMM and IMM, respectively). **Bottom**, Localization of IMS-GECO1.2 in ventricular myocytes, showing ring-like structures. **B**, Transmission electron micrographs of mitochondria in rat ventricular myocytes. Samples from rats injected with adeno-associated virus (AAV) 9-αMHC (alpha myosin heavy chain)-IMS-GECO1.2-APEX2 (ascorbate peroxidase 2) were treated with 3,3'-diaminobenzidine (DAB) chemical for 10 and 40 minutes. **Left**; 10-minute DAB treatment, demonstrating clear inner mitochondrial membranes and cristae. **Right**; The chemical reaction that occurs between the APEX2 tag and DAB leaves a dense particle in the IMS, indicating correct localization of IMS-GECO1.2 in the IMS. **C**, Representative recording of IMS Ca^{2+} in control ventricular myocyte (VM) expressing IMS-GECO1.2 subjected to field stimulation at 0.2, 0.5, and 2 Hz in the presence of 50-nmol/L isoproterenol (ISO). Pooled data for basal and peak $[Ca^{2+}]_{IMS}$ at 0.2 Hz (n=15) and 2 Hz (n=10). Data are presented as mean±SD, *P<0.05, 2-level random intercept model. N=6 control (3 female, 3 male) rats. **D**, Representative IMS-GECO1.2 (**left**) and cytosolic GECO1.2 (**right**) fluorescence recorded simultaneously in control VM treated with ISO for 5 minutes before pacing at 0.2 and 2 Hz. **E**, Superimposed traces of cytosolic GECO1.2 (black) and IMS GECO1.2 (blue) Ca^{2+}. **Center** and **Right**, Pooled data for time-to-peak and decay rate for cytosolic and IMS Ca^{2+}. Cytosolic: n=86, N=6 (2 male, 4 female) rats; IMS: n=40. N=7 (5 male, 2 female) rats. Two-level random intercept model. **F**, Representative IMS-GECO1.2 fluorescence recorded in control (black) and catecholaminergic polymorphic ventricular tachycardia (CPVT; red) ventricular myocytes. Myocytes were treated with ISO for 5 minutes before pacing at 2 Hz for 5 minutes. Two-level random intercept model. Control: n=12 cells, N=4 (3 female, 1 male) rats; CPVT: n=14 cells, N=6 (4 female, 2 male) rats.

demonstrating markedly different dynamics of cytosolic and IMS Ca^{2+} signals (Figure 3D). Given that genetic and chemical Ca^{2+} indicators can have significant differences in kinetics, we generated a cytosolic adenoviral GECO1.2 construct.[42] Importantly, by using the same probe with the same kinetics, one cytosolic, and one IMS-targeted, our data suggests that contrary to the established narrative, Ca^{2+} transients in the IMS do not, in fact, follow cytosolic

Ca^{2+} transients. Instead, Ca^{2+} in the IMS has a ≈50% slower time-to-peak and decay rate (Figure 3E; time-to-peak: *P=7.56×10^{-38}; cytosol: *P=9.90×10^{-30}). The latter explains why IMS Ca^{2+} accumulates upon increasing stimulation frequency.

Next, we assessed whether IMS-[Ca^{2+}] was different in isoproterenol-treated CPVT VMs compared with controls (Figure 3F). In control VMs, there is a significant accumulation of [Ca^{2+}] in the IMS, with an initial peak [Ca^{2+}] upon the start of electrical stimulation, followed by a steady state [Ca^{2+}] of 1 µmol/L. Importantly, IMS-[Ca^{2+}] is significantly increased in CPVT VMs, with an initial peak [Ca^{2+}] of 3.5 µmol/L and a steady state [Ca^{2+}] of 2 µmol/L (Figure 3F; initial: *P=0.002; steady state: *P=0.039). These data suggest that IMS-[Ca^{2+}] does not closely mirror cytosolic [Ca^{2+}] dynamics, but there is a significant accumulation of Ca^{2+} in this compartment under continuous periodic stimulation. In addition, these data suggest that under conditions of RyR2 hyperactivity post-β-adrenergic activation such as CPVT, there is increased [Ca^{2+}] in the IMS.

Increased IMS [Ca^{2+}] Evokes Calpain-Mediated Cleavage of Mitochondrial Structural Protein OPA1

We reasoned that a 2-fold increase in IMS-[Ca^{2+}] in CPVT could contribute to the changes observed in mitochondrial structure and ROS production through the activity of Ca^{2+}-dependent IMS µ-calpain, given that µ-calpain senses [Ca^{2+}] in the micromolar range.[45,46] Calpains are present in the cytosol and the mitochondria, and it is well established that their cysteine protease activity leads to cleavage of structural proteins such as JPH2 (junctophilin-2).[21,47,48] In mitochondria, OPA1 is a protein implicated in flattening of mitochondrial cristae.[49] Cleavage of OPA1 would change the structural integrity of the mitochondria and lead to widening of cristae, and we hypothesized that this may be a calpain target. Of note, expression of full-length OPA1 was significantly reduced in CPVT VMs compared with controls (Figure 4A, *P=0.004).

To test the hypothesis that RyR2-mediated SR Ca^{2+} leak may alter IMS calpain activity and, thus, expression of full-length OPA1 protein, we treated VMs isolated from control rat hearts with low-dose caffeine (200 µmol/L, 5 minutes) and isoproterenol (50 nmol/L, 5 minutes) and paced for 5 minutes at 2 Hz. Low-dose caffeine is known to increase RyR2 activity and has been used as an approach to mimic Ca^{2+} mishandling in CPVT.[4] Similar to our observations in CPVT VMs, we confirmed that this approach also increased IMS-[Ca^{2+}] and reduced matrix [Ca^{2+}] (Figure 4B and 4C). Isolated VMs treated with low-dose caffeine had reduced expression of full-length OPA1 protein (*P=0.004), and importantly, this reduction could be rescued by pretreatment with calpain inhibitors, MDL-28170 (5 µmol/L, 30 minutes; Figure 4D) and E64d (20 µmol/L, 30 minutes; Figure S11). There was no change in other documented or potential mitochondrial and cytosolic calpain targets (AIF [apoptosis-inducing factor] 1, MICU1, ANT (adenine nucleotide transporter), and JPH2).[21,47,48]

Next, to directly test whether OPA1 is a target of calpains, we performed a cleavage assay[50] using an N-terminal FLAG (peptide tag DYKDDDDK)–tagged, C-terminal HA–tagged OPA1 construct (Figure 4E). Lysates from these OPA1/HEK293 (human embryonic kidney 293) cells co-expressing calpain 1 (µ-calpain) or calpain 2 (M-calpain) plasmids were used for these assays in the presence and absence of Ca^{2+} and calpain inhibitor MDL-28170. Western blot analysis revealed several N-terminal and C-terminal OPA1 cleavage products in the presence of calpain, confirming that IMS structural protein OPA1 is indeed a target of this cysteine Ca^{2+}–dependent protease. Collectively, these data suggest that elevated IMS-[Ca^{2+}] in CPVT drives calpain-mediated cleavage of mitochondrial structural protein OPA1.

To confirm whether loss of full-length OPA1 had effects on ROS production and intracellular Ca^{2+} cycling, we knocked down OPA1 expression in control VMs using short hairpin RNA (shRNA) to mimic CPVT. Knockdown was confirmed by the Western blot (Figure 5A). Matrix ROS probe MLS-HyPer7 revealed that OPA1 shRNA significantly increased mitochondrial ROS emission (*P=1.0×10^{-4}), suggesting that the lack of full-length OPA1 protein does contribute to mitochondrial dysfunction (Figure 5B). The functional impact of changes in cristae structure morphology was previously ascribed to destabilization of electron transport chain (ETC) complexes, reducing the efficiency of oxidative phosphorylation and increasing mito-ROS emission.[51–55] Using blue native gel electrophoresis (BN-PAGE), we assessed the impact of OPA1 knockdown with shRNA on assembly of ETCs into large multimolecular supercomplexes, that is, respirasomes. Figure 5C demonstrates a significant reduction in bands of high molecular weight entities for complexes I (*P=0.026), III (*P=0.004), and IV (*P=0.023), confirming destabilization of ETC supercomplexes by OPA1 shRNA. OPA1 knockdown did not fully recapitulate the CPVT phenotype. In contrast to CPVT, isoproterenol-treated OPA1 knockdown VMs did not exhibit changes in Ca^{2+} transient amplitude and SR Ca^{2+} content measured using cytosolic Ca^{2+} indicator Fluo-3 (Figure 5D). However, OPA1 knockdown–mediated reduction in ETC supercomplexes was observed in parallel with an increase in spontaneous Ca^{2+} waves (*P=7.1×10^{-11}). These data indicate that loss of full-length OPA1 mediates changes in mitochondrial cristae structure that is associated with increased mitochondrial ROS emission, which subsequently evokes RyR2 dysfunction contributing to intracellular Ca^{2+} mishandling.

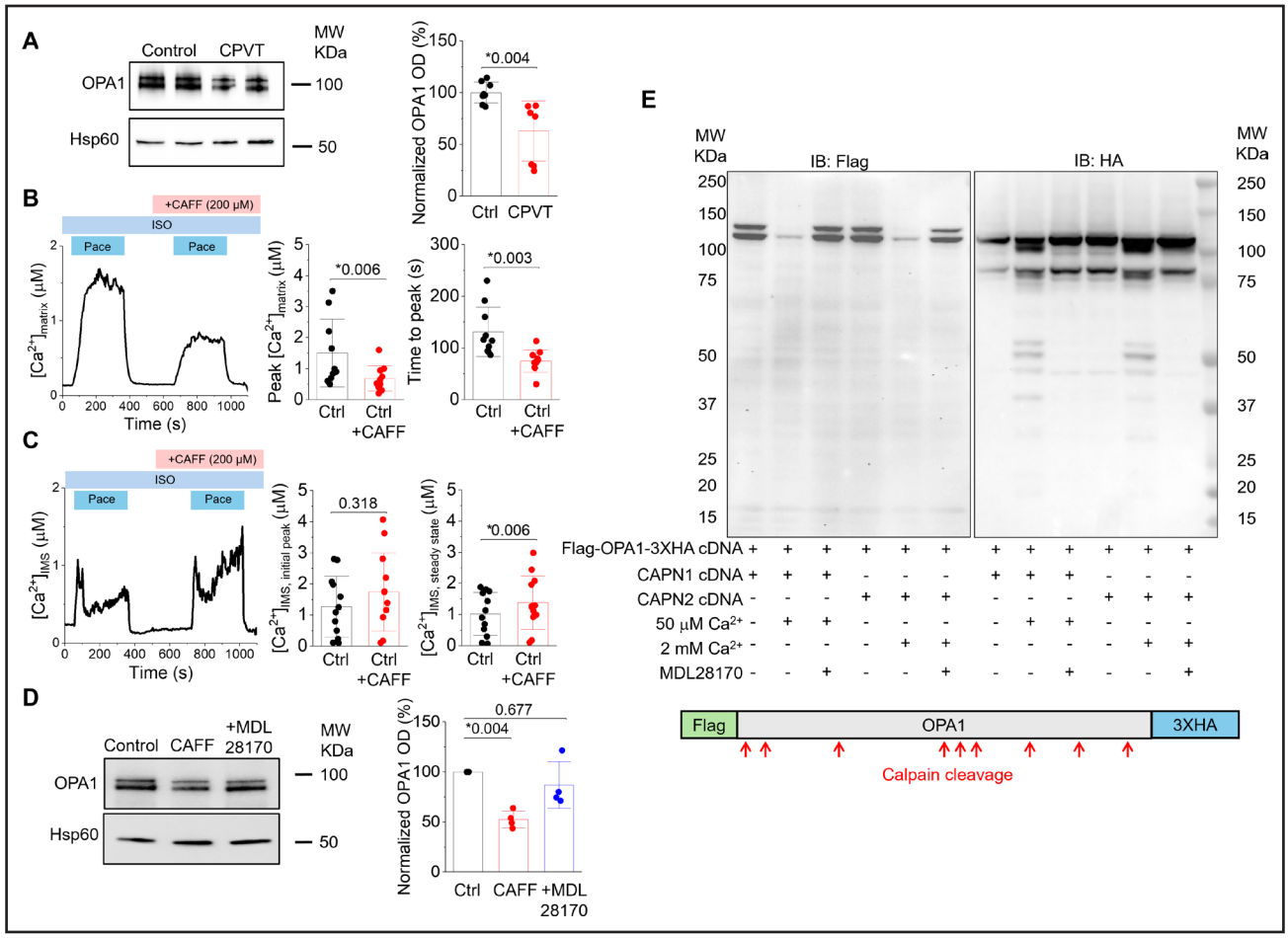

Figure 4. Increased [Ca^{2+}] in the intermembrane space evokes calpain-mediated cleavage of mitochondria structural protein OPA1 (optic atrophy protein 1).

A, Representative Western blot of optic atrophy 1 protein (OPA1) and Hsp60 (heat shock protein 60) and pooled data for OD normalized to Hsp60. Data are presented as mean±SD, **P*<0.05, Student *t* test. Control: N=8 (4 female, 4 male) rats; catecholaminergic polymorphic ventricular tachycardia (CPVT): N=8 (4 female, 4 male) rats. **B**, Representative mtRCamp1h fluorescence recorded in control ventricular myocyte, before and after application of low-dose caffeine (200 μmol/L) to evoke RyR2 (ryanodine receptor)–mediated sarcoplasmic reticulum (SR) Ca^{2+} leak. Myocytes were treated with isoproterenol (ISO; 50 nmol/L) for 5 minutes before pacing at 2 Hz for 5 minutes, followed by application of low-dose caffeine and pacing at 2 Hz for 5 minutes, Student *t* test. n=10 cells, N=4 (1 female, 3 male) rats. **C**, Representative intermembrane space (IMS)-GECO1.2 fluorescence recorded in control ventricular myocyte, before and after application of low-dose caffeine to promote RyR2-mediated SR Ca^{2+} leak. Myocytes were treated with ISO for 5 minutes before pacing at 2 Hz for 5 minutes, followed by application of low-dose caffeine and pacing at 2 Hz for 5 minutes, paired Student *t* test. n=12 cells, N=4 (3 female, 1 male) rats. **D**, Representative Western blots demonstrating OPA1 expression in control myocytes, normalized to Hsp60 expression. Myocytes were treated with ISO for 5 minutes and paced for 5 minutes (2 Hz) in the absence and presence of low-dose caffeine. A subset of caffeine-treated myocytes was also preincubated with calpain inhibitor MDL-28170 (10 μmol/L, 30 minutes) before processing, 1-way ANOVA with Bonferroni post hoc, N=4 (3 female, 1 male) rats. **E**, Western blot images demonstrating mitochondrial structural protein OPA1 are cleaved by calpain. An N-terminal FLAG (peptide DYKDDDDK)–tagged and C-terminal 3xHA (3x human influenza hemagglutinin protein)–tagged OPA1 construct was coexpressed in HEK293 (human embryonic kidney 293) cells with CAPN (calpain) 1 or CAPN2 for 24 hours. Cell lysates were in the presence or absence of Ca^{2+} (50 μmol/L or 2 mmol/L), as well as calpain inhibitor MDL-28170 (10 μmol/L) for 20 minutes before processing.

Preventing Calpain-Mediated OPA1 Cleavage in the IMS Restores Mitochondrial Structure Reducing Mito-ROS and Intracellular Ca^{2+} Mishandling

Given the significant role of OPA1 in mitochondrial cristae maintenance,[17,49] we next sought to determine whether inhibition of calpain-mediated OPA1 cleavage could offer protection against mitochondrial structural remodeling and aberrant SR Ca^{2+} release that we observed. We utilized CAST (calpastatin), an endogenous inhibitor of calpain that is expressed ubiquitously in cells.[56,57] To specifically inhibit the activity of calpain in the IMS, we again fused the first 140 amino acids of MICU1 to the N terminus of CAST.

To assess whether inhibition of IMS-resident calpain was protective at the cellular level, isolated CPVT VMs were infected with an adenovirus containing IMS-CAST-FLAG. After 48 hours in culture, expression was confirmed with the FLAG antibody. Importantly, full-length OPA1

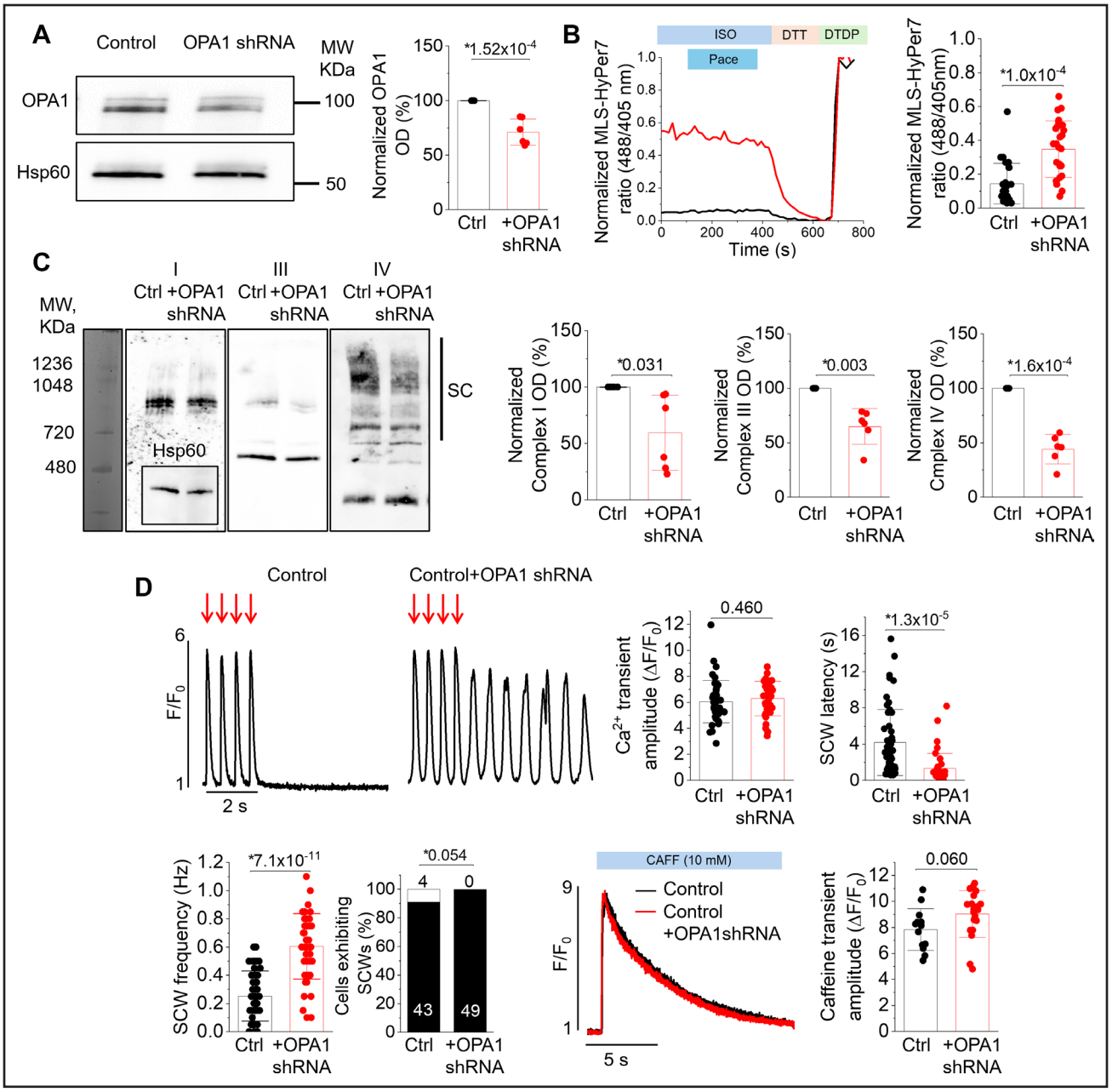

Figure 5. Knockdown of mitochondria structural protein OPA1 (optic atrophy protein 1) in healthy ventricular myocytes increases mito-reactive oxygen species (ROS) emission and leads to intracellular Ca^{2+} mishandling.
A, Representative Western blots demonstrating OPA1 and Hsp60 (heat shock protein 60) protein expression in control myocytes, and control myocytes expressing OPA1-short hairpin RNA (shRNA). The bar graph represents pooled data for OPA1 optical density (mean±SD). Hsp60 was used as a loading control. N=6 (3 male, 3 female), *P<0.05, paired Student t test. **B**, Representative MLS-HyPer7 mitochondrial ROS probe fluorescence recorded in control (black) and control+OPA1 shRNA (red) ventricular myocytes. Myocytes were treated with isoproterenol (ISO; 50 nmol/L) for 5 minutes before pacing at 2 Hz for 5 minutes. Fluorescence was normalized to minimum (dithiothreitol [DTT]; 5 mmol/L) and maximum (2,2′-dithiodipyridine [DTDP]; 200 µmol/L) fluorescence. Two-level random intercept model. Control: n=27 cells, N=6 (3 female, 3 male) rats; control+OPA1 shRNA: n=28 cells, N=4 (2 female, 2 male) rats. **C**, Representative BN-PAGE blots of electron transport chain complexes from control and control+OPA1 shRNA rat ventricular myocytes. Supercomplexes (SCs) are indicated by a black bar, paired Student t test. N=6 (3 female, 3 male) rats. **D**, Fluo-3 fluorescence (F/F_0) profiles of ventricular myocytes undergoing 2-Hz pace-pause protocol in the presence of ISO for assessment of intracellular Ca^{2+} handling and spontaneous Ca^{2+} waves (SCWs) and high-dose caffeine (10 mmol/L) treatment for assessment of sarcoplasmic reticulum (SR) Ca^{2+} content. Two-level random intercept model for Ca^{2+} transient amplitude and SCW latency, the Mann-Whitney U test for SCW frequency, and the Fisher exact test for cells exhibiting SCWs. Control: n=47 cells for Ca^{2+} transient amplitude, SCW frequency, and cells exhibiting SCWs, n=43 cells for SCW latency, n=13 cells for caffeine transient amplitude, N=8 (6 female, 2 male) rats; control+OPA1 shRNA: n=49 cells for Ca^{2+} transient amplitude, SCW latency, SCW frequency, and cells exhibiting SCWs, n=20 cells for caffeine transient amplitude, N=(2 female, 2 male).

expression was also increased in CPVT VMs expressing the construct versus nonexpressing CPVT controls (Figure 6A, *P=0.026). Furthermore, IMS-CAST expression restored ETC supercomplexes (Figure 6C, *P=0.005) and significantly attenuated mitochondrial ROS emission in CPVT VMs (Figure 6B, *P=0.002). Inhibition of IMS

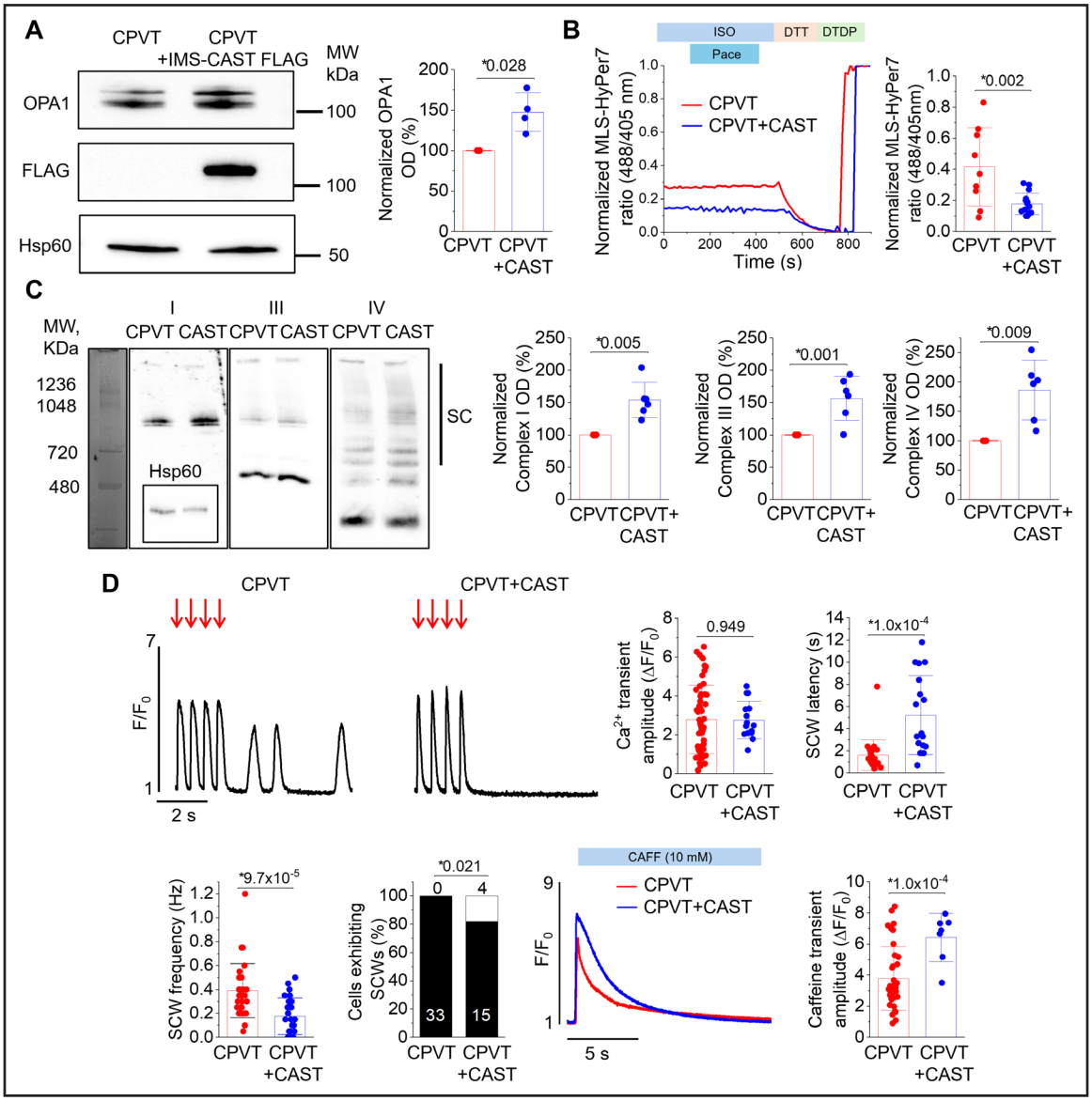

Figure 6. Expression of calpain inhibitor CAST (calpastatin) in the intermembrane space (IMS) reduces mito-reactive oxygen species (ROS) emission and normalizes intracellular Ca^{2+} handling in catecholaminergic polymorphic ventricular tachycardia (CPVT) ventricular myocytes.

A, Representative Western blot images demonstrating expression of IMS-CAST-FLAG (peptide DYKDDDDK-tag) in CPVT ventricular myocytes, visualized by a band when probed for FLAG expression. Bar graph represents pooled data for optical density for OPA1 (optic atrophy protein 1; mean±SD). Hsp60 (heat shock protein 60) was used as a loading control. N=4 (2 male, 2 female), *P<0.05, paired Student t test. **B**, Representative MLS-HyPer7 mitochondrial ROS probe fluorescence recorded in CPVT (red) and CPVT+IMS-CAST (blue) expressing ventricular myocytes. Myocytes were treated with isoproterenol (ISO; 50 nmol/L) for 5 minutes before pacing at 2 Hz for 5 minutes. Fluorescence was normalized to minimum (dithiothreitol [DTT]; 5 mmol/L) and maximum (2,2′-dithiodipyridine [DTDP]; 200 µmol/L) fluorescence. Two-level random intercept model. CPVT: n=9 cells, N=4 animals (2 female, 2 male); CPVT+CAST n=16 cells, N=3 animals (1 female, 2 male). **C**, Representative BN-PAGE blots of electron transport chain complexes from CPVT and CPVT+IMS-CAST rat ventricular myocytes. Supercomplexes (SCs) are indicated by a black bar, paired Student t test. N=6 CPVT (3 female, 3 male) rats. **D**, Fluo-3 fluorescence (F/F_0) profiles of ventricular myocytes undergoing 2-Hz pace-pause protocol in the presence of ISO for assessment of intracellular Ca^{2+} handling and spontaneous Ca^{2+} waves (SCWs) and high-dose caffeine (CAFF, 10 mmol/L) treatment for assessment of sarcoplasmic reticulum (SR) Ca^{2+} content. Two-level random intercept model for Ca^{2+} transient amplitude and SCW latency, the Mann-Whitney U test for SCW frequency, and the Fisher exact test for cells exhibiting SCWs. CPVT: n=33 cells for Ca^{2+} transient amplitude, SCW latency, SCW frequency, and cells exhibiting SCWs, n=36 cells for caffeine transient amplitude, N=8 (4 female, 4 male) rats; CPVT+CAST short hairpin RNA (shRNA): n=19 cells for Ca^{2+} transient amplitude, SCW frequency, and cells exhibiting SCWs, n=15 cells for SCW latency, n=7 cells for caffeine transient amplitude, N=4 (2 female, 2 male) rats.

calpain also improved intracellular Ca^{2+} handling, significantly delaying the onset of spontaneous Ca^{2+} waves to occur in CPVT VMs (Figure 6D, $^*P=1.0\times10^{-4}$). Of note, this improvement in Ca^{2+} homeostasis evoked by IMS-CAST occurs although there is still a gain-of-function mutation in the RyR2 channel, suggesting that mitochondrial remodeling and dysfunction are significant contributors to the arrhythmogenic phenotype of CPVT.

We reasoned that the restoration of ETC supercomplexes and functional improvements in CPVT VMs expressing IMS-CAST were due to reduced OPA1 cleavage and, thus, a reduction in cristae diameter. To assess this, we generated AAV9-IMS-CAST and injected rats in vivo via the tail vein with 10^{12} viral particles, before assessing hearts by transmission electron microscopy 4 weeks later (Figure 7A). Importantly, inhibition of calpain in the IMS via IMS-CAST expression reduced cristae diameter in CPVT VMs, indicating that calpain-mediated OPA1 cleavage indeed contributes to structural remodeling of mitochondria in CPVT hearts.

Inhibition of Calpain in the Mitochondrial IMS Attenuates Arrhythmic Potential

Finally, to test directly whether IMS calpain inhibition could reduce arrhythmic potential not just at the cellular level, but in the whole heart, we performed ex vivo optical mapping experiments (Figure 7B through 7H). CPVT rats were injected with AAV9-αMHC-IMS-CAST (10^{12} viral particles per rat, tail vein), and 4 weeks postinjection, hearts were removed for study. Langendorff-perfused hearts were stained with voltage-sensitive dye Di-4-ANEPPS and challenged with 100-nmol/L isoproterenol.[58] This protocol did not elicit arrhythmias in hearts from control littermates. Hearts from CPVT animals demonstrated rare spontaneous VT. To gain insight into mechanisms of VT initiation, hearts were subjected to a standard arrhythmia challenge rapid pacing protocol. Arrhythmia was evoked by short bouts of fast pacing (5–15 stimuli at 100-ms cycle length). As presented in Figure 7B through 7H, VT was triggered by focal activity, with focal activity distributed randomly in a classical CPVT pattern. We did not find differences in conduction velocity and action potential duration between groups (Figure 7G), suggesting a lack of gross structural changes of cardiac tissue in CPVT, in line with previous reports.[9,33,34] Importantly, IMS-CAST expression eliminated VT in Langendorff-perfused isoproterenol-challenged RyR2-S2236L$^{(+/-)}$ hearts, highlighting the key role of IMS calpain activation for arrhythmogenesis in CPVT.

DISCUSSION

In this study, using a novel rat model and a new genetic tool, we demonstrate a new mechanism, whereby pathological enhancement of RyR2 activity contributes to mitochondrial damage by increasing Ca^{2+} in the mitochondrial IMS. Thus, our work challenges the dogma that IMS-[Ca^{2+}] is equivalent to cytosolic [Ca^{2+}]. We found that an increase in IMS-[Ca^{2+}] driven by RyR2 hyperactivity promotes calpain-mediated degradation of OPA1. This causes structural changes in cristae organization, resulting in destabilization of ETC supercomplexes and an exacerbation of mito-ROS production and proarrhythmic RyR2 activity (Figure 8).

A new rat model of CPVT was used in this study to define the effects of RyR2 hyperactivity on mitochondrial structure and ROS production (Figure 1). Importantly, our new RyR2-S2236L$^{(+/-)}$ rat model recapitulates key features of CPVT pathogenesis and phenotype in humans,[6] demonstrating no overt functional and structural changes of the heart (Figure S2; Table S2). In vivo rats injected with epinephrine and caffeine demonstrate bidirectional polymorphic VT, a hallmark of clinically presenting CPVT (Figure 1B and 1C). Ex vivo membrane potential optical mapping experiments corroborate that VT is triggered by focal activity in CPVT hearts (Figure 7B). Isolated CPVT VMs challenged with isoproterenol show spontaneous RyR2-mediated SR Ca^{2+} release (Figures 1D and 6D; Figure S4) that underlies delayed afterdepolarizations and extra-systolic APs (Figure 1D). Thus, the model used in this study provides an opportunity to study the effects of RyR2 gain of function on mitochondrial structure and its impact on arrhythmogenesis.

Abnormally high RyR2 activity and defective mitochondria are common parallel findings in CVDs.[3–5,15,59–62] Increased mitochondrial ROS production in diseased hearts affects RyR2 directly via oxidation of reactive cysteines of the channel[4,63–65] or indirectly, via oxidation of CaMKII, which subsequently promotes its phosphorylation of RyR2 at Serine-2814.[66–68] Substantial evidence suggests that both these modifications pathologically increase RyR2 activity. More recent studies suggest that hyperactive RyR2s can also affect mitochondria as well, and partial RyR2 inhibition can prevent its pathological consequences.[4,5,69,70] Consistent with previous reports, here, we found that mito-ROS and RyR2 oxidation are increased (Figure 2A and 2B), while mitochondrial matrix [Ca^{2+}] is reduced in CPVT rat VMs under β-adrenergic stimulation (Figure 2C). Changes in matrix [Ca^{2+}] can affect ATP production by altering activities of several mitochondrial Ca^{2+}–dependent dehydrogenases that control production rates of NADH (reduced nicotinamide adenine dinucleotide) and $FADH_2$ (reduced flavin adenine dinucleotide) and, thereby, activity of the electron transport chain.[71,72] However, the exact mechanisms linking changes in mito-Ca^{2+} and pathological mito-ROS production remain elusive. Furthermore, our experiments demonstrate that mito-ROS is already increased in CPVT VMs under basal conditions (Figure S7), where low matrix [Ca^{2+}] levels in CPVT VMs are indistinguishable from controls (Figure S8). This suggests severe lasting damage

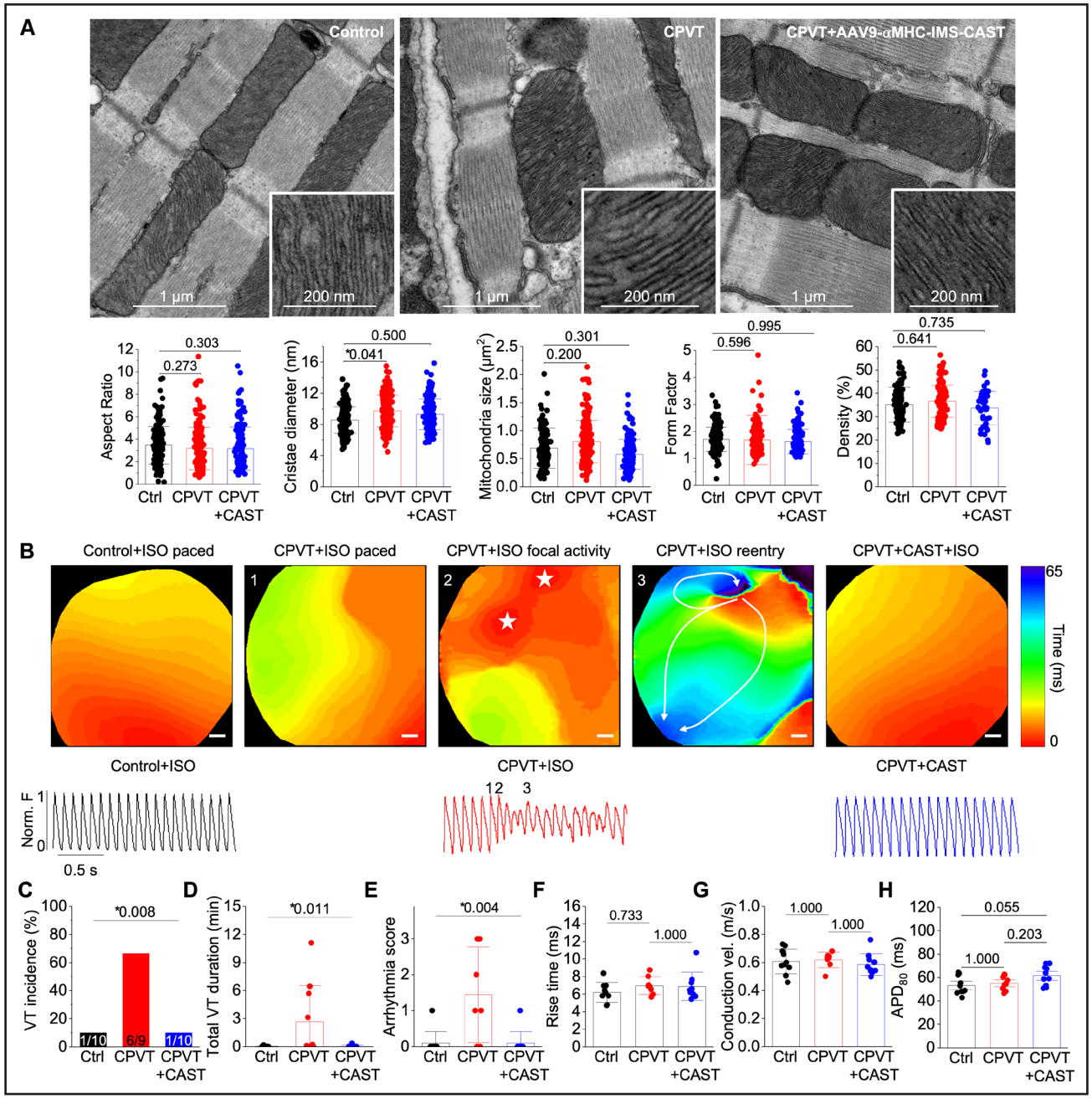

Figure 7. Endogenous calpain activity in the intermembrane space contributes to mitochondrial structural remodeling and arrhythmia in catecholaminergic polymorphic ventricular tachycardia (CPVT).

A, Representative transmission electron micrographs of ventricular myocytes from control, CPVT, and CPVT rats injected with intermembrane space–targeted calpain inhibitor calpastatin (adeno-associated virus [AAV] 9-αMHC (alpha myosin heavy chain)-intermembrane space [IMS]-CAST [calpastatin]). Hearts were removed from rats 4 weeks after injection and fixed in 2.5% glutaraldehyde solution. Data are presented as mean±SD, **P*<0.05, 2-level random intercept model. Control: N=6 (3 female, 3 male) rats; CPVT: N=7 (5 female, 2 male) rats; and CPVT+CAST: N=4 (2 female, 2 male) rats. **B** and **C**, Representative activation maps (**A**) and corresponding action potentials (**B**) at 100-ms pacing frequency under 100-nmol/L isoproterenol (ISO). Scale bar for activation map=1 mm. CPVT hearts showed focal activity (*), which initiated the formation of reentry (white arrows) under fast pacing. Numbers 1 to 3 on activation maps indicate the time point in action potential traces. **C**, Ventricular tachycardia (VT) incidence (%). Freeman-Halton extension of the Fisher exact probability test. **D**, Total VT duration (minutes), Kruskal-Wallis ANOVA. **E**, An arrhythmia score based on the most severe arrhythmia was applied: no arrhythmias=0; nonsustained VT (<30 s)=1; sustained VT (>30 s)=2; and nonterminating VT=3. VT was defined as ≥3 consecutive premature ventricular complexes, Kruskal-Wallis ANOVA. **F**, Rise time (ms), 1-way ANOVA with Bonferroni post hoc. **G**, Conduction velocity (m/s), 1-way ANOVA with Bonferroni post hoc. **H**, Action potential duration, APD_{80} (ms), 1-way ANOVA with Bonferroni post hoc. N for ex vivo optical mapping experiments: control: N=10 (4 female, 6 male); CPVT: N=9 (4 female, 5 male) rats; and CPVT+CAST: N=10 (4 female, 6 male) rats.

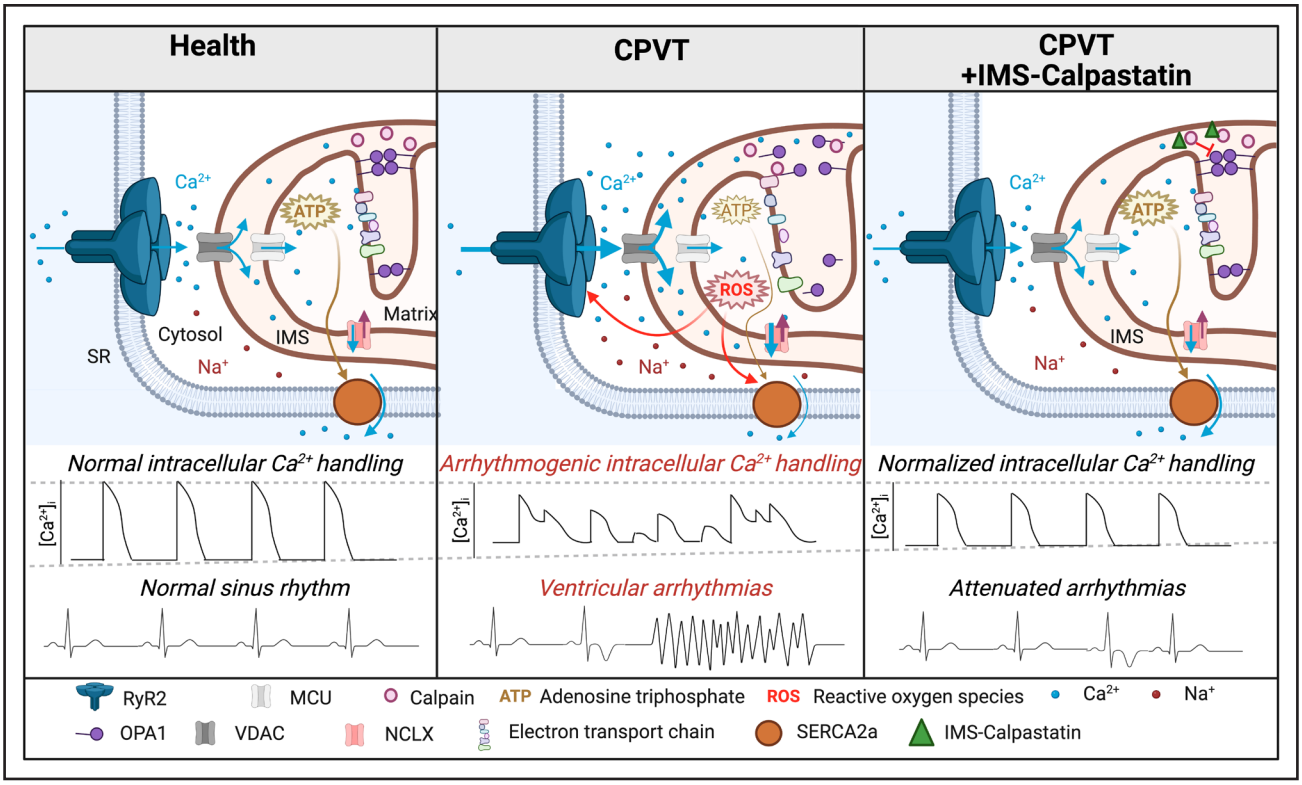

Figure 8. Schematic of proposed mechanism.
Enhancement of RyR2 (ryanodine receptor) activity contributes to mitochondrial dysfunction by facilitating Ca^{2+} accumulation in the mitochondrial intermembrane space (IMS). RyR2-driven increase in cytosolic Ca^{2+} during diastole promotes intracellular Na^+ overload, reducing mitochondria matrix Ca^{2+} retention capacity due to increased NCLX (mitochondrial $Na^+/Ca^{2+}/Li^+$ exchanger) activity. Reciprocal increase in IMS-$[Ca^{2+}]$ promotes calpain-dependent degradation of OPA1 (optic atrophy protein 1). It causes structural changes in cristae organization, resulting in destabilization of electron transport chain (ETC) supercomplexes, which increases mito-reactive oxygen species (ROS) production, exacerbating proarrhythmic RyR2 dysfunction. Inhibition of IMS calpain by expressing IMS-targeted calpastatin restores cristae architecture and ETC supercomplexes. It reduces mito-ROS mishandling, attenuating RyR2 dysfunction, thereby preventing proarrhythmic spontaneous sarcoplasmic reticulum Ca^{2+} release. The image was made with Biorender.

of CPVT mitochondria beyond its impaired ability to retain matrix Ca^{2+} under acute β-adrenergic stimulation. Attempts to restore matrix $[Ca^{2+}]$ by pharmacologically enhancing or genetically overexpressing MCU led to disparate results. In some cases, protection and restoration of ROS homeostasis are evidenced[15,16,73,74] while being ineffective in others.[4,12,13,73,75] Furthermore, approaches designed to reduce MCU activity and, thereby, promote subsequent reduction in matrix $[Ca^{2+}]$ did not produce deleterious effects.[27,76,77] On the contrary, it displayed reduced mito-ROS production.[4,12,13,78] Together, these data suggest that reduced matrix $[Ca^{2+}]$ is unlikely to be the major cause of increased ROS production by mitochondria in diseased hearts.

The main source of ROS in mitochondria is the ETC.[79] ETC complexes are located in mitochondrial cristae, and their compact organization is pivotal for ETC efficiency.[53,80,81] Importantly, many structural proteins that are critical for cristae formation and stabilization are found in the mitochondrial IMS. The dynamin-related protein OPA1 is one such protein central for maintaining cristae morphology, with the long, IMM-bound isoform forming tight cristae junctions, while the short isoform is soluble. Downregulation of OPA1 is associated with reduced respiration due to a reduction in stabilized ETC supercomplexes and increased mito-ROS production.[53,55,81] Proteolysis of OPA1 by proapoptotic proteins leads to adverse consequences.[26] However, whether impaired Ca^{2+} handling can affect OPA1 integrity remained unknown. Importantly, the major protease μ-calpain, activated when $[Ca^{2+}]$ reaches micromolar range, was found in the mitochondrial IMS.[20,21] The current consensus is that IMS-$[Ca^{2+}]$ is equal to $[Ca^{2+}]$ in cytosol, given the high permeability of the OMM to the ion.[19] Should this be the case in the heart, IMS calpain activation in VMs would be unlikely other than in conditions such as ischemia-reperfusion injury, where massive intracellular Ca^{2+} overload reaches the micromolar range for long periods of time.[82] Using a newly designed IMS-Ca^{2+} biosensor, our new data have challenged this dogma. Our experiments using an IMS-GECO1.2 clearly demonstrated that in isoproterenol-treated, periodically paced VMs, IMS-$[Ca^{2+}]$ reaches micromolar range (Figure 3C through 3E). The main route for Ca^{2+} to enter and leave intermitochondrial space is VDAC, a highly expressed

anion channel in the OMM that transports small molecules including ATP.[19,83] VDAC transduces a wide variety of cellular inputs, and importantly, its activity exhibits strong dependence upon cytosolic [Ca^{2+}]. In detailed work using rat liver isolated mitochondria, the Hajnóczky group showed that Ca^{2+} permeability of VDAC is minuscule at low [Ca^{2+}]cyt.[84] VDAC Ca^{2+} permeability increases several-fold at supramicromolar [Ca^{2+}], which is within the range that cytosolic [Ca^{2+}] reaches at the peak of Ca^{2+} transient in VMs under β-adrenergic stimulation.[15,69,85] Critically, cytosolic [Ca^{2+}] drops rapidly upon cessation of SR Ca^{2+} release in VMs, which must lead to an abrupt reduction in VDAC Ca^{2+} permeability, effectively entrapping Ca^{2+} in IMS for longer, as evidenced by the comparison of the dynamics of cytosolic and IMS transients recorded using the same biosensor GECO1.2 expressed cytosol and IMS, respectively (Figure 3E). Accordingly, we found substantial accumulation of IMS-[Ca^{2+}] upon increasing stimulation frequency in VMs treated with isoproterenol (Figure 3B and 3C). Moreover, we found augmented IMS Ca^{2+} accumulation in conditions promoting spontaneous RyR2-mediated SR Ca^{2+} release both under pharmacological intervention with low-dose caffeine (Figure 4B) or in our genetic gain-of-RyR2 function model (Figure 3F).

In addition, we found a significant reduction in the capacity of mitochondria to accumulate Ca^{2+} in the matrix in CPVT VMs (Figure 2C) and in control VMs treated with low-dose caffeine (Figure 4B). Previously, it was shown that there is a steep Ca^{2+} dependency of MCU-mediated uptake in cardiomyocytes.[86] Therefore, MCU-mediated Ca^{2+} uptake is negligible in periodically stimulated VMs under basal conditions, despite a strong driving force through heavily charged IMM (Figure S7). Uptake becomes pronounced upon β-adrenergically induced increase in cytosolic Ca^{2+} transients.[4] Our experiments using permeabilized VMs expressing mtRCamp1h confirmed steep Ca^{2+} dependence of mitochondrial matrix Ca^{2+} uptake (Figure S8). However, we found that application of as little as 200 nmol/L [Ca^{2+}] into the bath solution is sufficient for uptake initiation, consistent with an earlier estimation by the Bers group.[87] Thus, diminished Ca^{2+} transient amplitude at elevated diastolic Ca^{2+} levels in CPVT cannot fully explain the pronounced decrease in matrix [Ca^{2+}] in diseased isoproterenol-treated VMs. Furthermore, immunoblot analysis demonstrates a significant decrease in levels of MICU1 (Figure 2E), a negative regulator of MCU, which would be expected to increase MCU activity in CPVT.[40] Apparently, this adaptive change is insufficient to overcome the loss of matrix [Ca^{2+}]. In addition, MICU1 has been established as another regulator of cristae architecture.[88] This could suggest that not the loss from the MCU complex, but mitochondrial structural change may underlie MICU1 expression levels' reduction in CPVT VMs. We reasoned that the reduced capacity of the matrix to retain Ca^{2+} stems from the increased activity of NCLX due to cellular Na^+ overload.[15,41,61] Our experiments using Na^+-sensitive dye demonstrate a significant increase in cytosolic [Na^+] in paced CPVT VMs in the presence of isoproterenol (Figure S9). Furthermore, reduction of Na^+ overload in CPVT VMs by attenuation of intracellular Ca^{2+} mishandling by scavenging of mitochondria ROS[4,13] restored the ability of mitochondria to accumulate Ca^{2+} in the matrix (Figure S10). Na^+-dependent reduction of mitochondria's ability to retain Ca^{2+} in its matrix could be the major contributor to the increased Ca^{2+} in IMS in diseased VMs.

Of note, the increase in IMS-[Ca^{2+}] in CPVT VMs was accompanied by decreased OPA1 levels (Figure 4A). Furthermore, acute hyperactivation of RyR2 mirrored the results obtained in CPVT myocytes, significantly decreasing levels of OPA1, which was prevented by preincubation of VMs with pharmacological calpain inhibitors MDL-28170 (Figure 4D) and E64d (Figure S11). Experiments in a heterologous system confirmed OPA1 as a bona fide calpain target (Figure 4E). Importantly, transmission electron microscopy experiments revealed cristae widening in CPVT heart samples, which was attenuated by AAV-mediated expression of IMS-targeted CAST, an endogenous calpain inhibitor[57] (Figure 7A). Together, these data provide new mechanistic insight into the dynamics between intracellular Ca^{2+} homeostasis in CVD and modulation of mitochondrial structure.

Emerging evidence suggests that calpains may be promising therapeutic targets to treat various forms of CVD. Pharmacological inhibition of cytosolic calpains showed improvement of Ca^{2+}-induced Ca^{2+} release in hypertrophy and HF by reversing loss of tight contacts between SR and T-tubules due to calpain-dependent proteolysis of a dyadic structural protein JPH2.[48] Furthermore, inhibition or genetic knock-out of calpain was shown to significantly reduce post-ischemia-reperfusion injury, improving mitochondria function and reducing mito-ROS production.[89] Of note, calpain loss of function was protective in less extreme conditions such as the aged heart or pharmacologically induced ER stress.[23,90] Both aging and ER stress were associated with a proarrhythmic increase in RyR2 activity due to channel oxidation.[3,69] Our data demonstrate that direct inhibition of calpain in the IMS with CAST reduces mito-ROS production and markedly suppresses proarrhythmic spontaneous Ca^{2+} waves in isolated CPVT VMs (Figure 6). Importantly, calpain inhibition increased OPA1 levels in CPVT VMs, while OPA1 knockdown using shRNA increased mito-ROS, promoting spontaneous RyR2-mediated SR Ca^{2+} release in VMs from control hearts (Figure 5). This further corroborates the important role of Ca^{2+}-calpain–dependent degradation of OPA1 in proarrhythmic feedback of mitochondria on RyR2 function via ROS. At the tissue level, RyR2-mediated Ca^{2+} mishandling in RyR2-S2236L$^{(+/-)}$ hearts was associated with

focal activity evolving into VT under catecholaminergic stimulation, a hallmark of CPVT (Figure 7B). Importantly, AAV9-mediated expression of IMS-targeted CAST dramatically reduced arrhythmogenicity in CPVT rat hearts. This suggests that Ca^{2+}-dependent mitochondria damage, secondary to RyR2 gain-of-function mutation, plays a pivotal role in arrhythmia precipitation. Furthermore, our findings have much broader implications for various forms of CVD accompanied by increased RyR2 activity and, thus, high arrhythmic potential, including HF or age-dependent cardiac dysfunction.

To summarize, our data suggest that RyR2 hyperactivity increases [Ca^{2+}] in the mitochondrial IMS. This drives IMS calpain–mediated proteolysis of OPA1 and evokes disruption of mitochondrial cristae, loss of ETC supercomplexes, and excessive release of damaging ROS. Critically, this contributes to RyR2 hyperactivation and ventricular tachyarrhythmia. Therefore, attenuating intracellular Ca^{2+} mishandling in diseased hearts by targeting IMS calpain may be beneficial in patients at risk of sudden cardiac death.

ARTICLE INFORMATION

Received May 23, 2025; revision received September 29, 2025; accepted October 2, 2025.

Affiliations

Department of Physiology and Cell Biology (S.H., R.T., R.V., F.P., S.G., A.E.B., D.T.) and Division of Cardiac Surgery, Department of Surgery, College of Medicine (M.W.G.), The Ohio State University, Columbus. College of Medicine, Dorothy M. Davis Heart and Lung Research Institute, The Ohio State University Wexner Medical Center, Columbus (S.H., R.T., R.V., F.P., M.W.G., S.G., A.E.B., D.T.). Department of Cellular and Molecular Medicine, The University of Arizona, Tucson (S.H., S.Q., R.B.). Department of Pathology, Anatomy and Cell Biology, MitoCare Center, Thomas Jefferson University, Philadelphia, PA (Z.N., G.C.). Faculty of Medicine, Health and Life Sciences, Swansea University, Wales, United Kingdom (M.B., C.H.G.). Division of Cardiovascular Medicine, Department of Internal Medicine, Abboud Cardiovascular Research Center, Carver College of Medicine, University of Iowa (J.W.). Department of Medicine, Cardiovascular Research Center, Rhode Island Hospital, The Warren Alpert Medical School of Brown University, Providence (B.-R.C.).

Acknowledgments

The authors thank the University of Michigan Transgenic Core for the generation of RyR2 (ryanodine receptor) mutant rats.

Author Contributions

S. Hamilton was involved in conceptualization, data curation, formal analysis, funding acquisition, investigation, methodology, supervision, writing-original draft preparation, and writing-review and editing. R. Terentyeva was involved in investigation, formal analysis, and writing-review and editing. R. Veress was involved in investigation and formal analysis. F. Perger was involved in investigation and formal analysis. Z. Nichtova was involved in investigation. M. Bannister was involved in investigation, funding acquisition, and writing-review and editing. J. Wang was involved in investigation. S. Quiggle was involved in investigation. R. Battershell was involved in investigation. M.W. Gorr was involved in investigation, formal analysis, and writing-review and editing. S. Györke was involved in funding acquisition, resources, and writing-review and editing. B.-R. Choi was involved in formal analysis and writing-review and editing. C.H. George was involved in investigation, funding acquisition, and writing-review and editing. A.E. Belevych was involved in investigation, formal analysis, and writing-review and editing. G. Csordás was involved in investigation, formal analysis, resources, and writing-review and editing. D. Terentyev was involved in conceptualization, data curation, formal analysis, funding acquisition, investigation, methodology, supervision, writing-original draft preparation, and writing-review and editing.

Sources of Funding

This work was supported by grants from the National Institutes of Health (NIH) National Heart, Lung, and Blood Institute (NHLBI) R00HL155492 (to S. Hamilton), NIH NHLBI R01HL167963 (to M.W. Gorr) NIH NHLBI R01HL063043, NIH NHLBI R01HL074045, and NIH NHLBI R01HL138579 (to S. Györke), NIH NHLBI R01HL122124, NIH NHLBI R01HL142864, and NIH National Institute of Diabetes and Digestive and Kidney Diseases R01DK125897 (to G. Csordás), NIH NHLBI R01HL166604, NIH NHLBI R01HL142588, and NIH NHLBI R03TR004471 (to D. Terentyev), the American Heart Association (AHA) Postdoctoral Fellowship 916348 (to R. Veress), the AHA Transformational Project Award 24TPA1293486 (to D. Terentyev) and 25TPA1468455 (https://doi.org/10.58275/AHA.25TPA1468455.pc.gr.233968; to S. Hamilton), the Harold S. Geneen Charitable Trust Awards Program for Coronary Heart Disease Research (to S. Hamilton), the University of Arizona Sarver Heart Center (to S. Hamilton), the British Heart Foundation RG/15/6/31436 (to C.H. George and M. Bannister), and a Welsh Government Infrastructure Award (to C. George and M. Bannister).

Disclosures

None.

Supplemental Material

Supplemental Materials and Methods
Tables S1–S2
Figures S1–S11
Major Resources Table
References 91–95

REFERENCES

1. Hamilton S, Terentyeva R, Clements RT, Belevych AE, Terentyev D. Sarcoplasmic reticulum-mitochondria communication; implications for cardiac arrhythmia. *J Mol Cell Cardiol.* 2021;156:105–113. doi: 10.1016/j.yjmcc.2021.04.002
2. Brown DA, O'Rourke B. Cardiac mitochondria and arrhythmias. *Cardiovasc Res.* 2010;88:241–249. doi: 10.1093/cvr/cvq231
3. Cooper LL, Li W, Lu Y, Centracchio J, Terentyeva R, Koren G, Terentyev D. Redox modification of ryanodine receptors by mitochondria-derived reactive oxygen species contributes to aberrant Ca2+ handling in ageing rabbit hearts. *J Physiol.* 2013;591:5895–5911. doi: 10.1113/jphysiol.2013.260521
4. Hamilton S, Terentyeva R, Martin B, Perger F, Li J, Stepanov A, Bonilla IM, Knollmann BC, Radwański PB, Györke S, et al. Increased RyR2 activity is exacerbated by calcium leak-induced mitochondrial ROS. *Basic Res Cardiol.* 2020;115:38. doi: 10.1007/s00395-020-0797-z
5. Santulli G, Xie W, Reiken SR, Marks AR. Mitochondrial calcium overload is a key determinant in heart failure. *Proc Natl Acad Sci USA.* 2015;112:11389–11394. doi: 10.1073/pnas.1513047112
6. Priori SG, Napolitano C, Memmi M, Colombi B, Drago F, Gasparini M, DeSimone L, Coltorti F, Bloise R, Keegan R, et al. Clinical and molecular characterization of patients with catecholaminergic polymorphic ventricular tachycardia. *Circulation.* 2002;106:69–74. doi: 10.1161/01.cir.0000020013.73106.d8
7. Bongianino R, Denegri M, Mazzanti A, Lodola F, Vollero A, Boncompagni S, Fasciano S, Rizzo G, Mangione D, Barbaro S, et al. Allele-specific silencing of mutant mRNA rescues ultrastructural and arrhythmic phenotype in mice carriers of the R4496C mutation in the ryanodine receptor gene (*RYR2*). *Circ Res.* 2017;121:525–536. doi: 10.1161/CIRCRESAHA.117.310882
8. Lavorato M, Iyer VR, Dewight W, Cupo RR, Debattisti V, Gomez L, De la Fuente S, Zhao YT, Valdivia HH, Hajnóczky G, et al. Increased mitochondrial nanotunneling activity, induced by calcium imbalance, affects intermitochondrial matrix exchanges. *Proc Natl Acad Sci USA.* 2017;114:E849–E858. doi: 10.1073/pnas.1617788113
9. Cerrone M, Napolitano C, Priori SG. Catecholaminergic polymorphic ventricular tachycardia: a paradigm to understand mechanisms of arrhythmias associated to impaired Ca(2+) regulation. *Heart Rhythm.* 2009;6:1652–1659. doi: 10.1016/j.hrthm.2009.06.033
10. Garcia-Dorado D, Ruiz-Meana M, Inserte J, Rodriguez-Sinovas A, Piper HM. Calcium-mediated cell death during myocardial reperfusion. *Cardiovasc Res.* 2012;94:168–180. doi: 10.1093/cvr/cvs116
11. García-Rivas GJ, Carvajal K, Correa F, Zazueta C. Ru360, a specific mitochondrial calcium uptake inhibitor, improves cardiac post-ischaemic functional recovery in rats in vivo. *Br J Pharmacol.* 2006;149:829–837. doi: 10.1038/sj.bjp.0706932

12. Hamilton S, Terentyeva R, Kim TY, Bronk P, Clements RT, O-Uchi J, Csordás G, Choi BR, Terentyev D. Pharmacological modulation of mitochondrial Ca^{2+} content regulates sarcoplasmic reticulum Ca^{2+} release via oxidation of the ryanodine receptor by mitochondria-derived reactive oxygen species. *Front Physiol*. 2018;9:1831. doi: 10.3389/fphys.2018.01831
13. Hamilton S, Terentyeva R, Perger F, Hernández Orengo B, Martin B, Gorr MW, Belevych AE, Clements RT, Györke S, Terentyev D. MCU overexpression evokes disparate dose-dependent effects on mito-ROS and spontaneous Ca^{2+} release in hypertrophic rat cardiomyocytes. *Am J Physiol Heart Circ Physiol*. 2021;321:H615–H632. doi: 10.1152/ajpheart.00126.2021
14. Liu T, Takimoto E, Dimaano VL, DeMazumder D, Kettlewell S, Smith G, Sidor A, Abraham TP, O'Rourke B. Inhibiting mitochondrial Na+/Ca2+ exchange prevents sudden death in a Guinea pig model of heart failure. *Circ Res*. 2014;115:44–54. doi: 10.1161/CIRCRESAHA.115.303062
15. Liu T, Yang N, Sidor A, O'Rourke B. MCU overexpression rescues inotropy and reverses heart failure by reducing SR Ca^{2+} leak. *Circ Res*. 2021;128:1191–1204. doi: 10.1161/CIRCRESAHA.120.318562
16. Suarez J, Cividini F, Scott BT, Lehmann K, Diaz-Juarez J, Diemer T, Dai A, Suarez JA, Jain M, Dillmann WH. Restoring mitochondrial calcium uniporter expression in diabetic mouse heart improves mitochondrial calcium handling and cardiac function. *J Biol Chem*. 2018;293:8182–8195. doi: 10.1074/jbc.RA118.002066
17. Pernas L, Scorrano L. Mito-morphosis: mitochondrial fusion, fission, and cristae remodeling as key mediators of cellular function. *Annu Rev Physiol*. 2016;78:505–531. doi: 10.1146/annurev-physiol-021115-105011
18. Osman C, Merkwirth C, Langer T. Prohibitins and the functional compartmentalization of mitochondrial membranes. *J Cell Sci*. 2009;122:3823–3830. doi: 10.1242/jcs.037655
19. Rosencrans WM, Rajendran M, Bezrukov SM, Rostovtseva TK. VDAC regulation of mitochondrial calcium flux: from channel biophysics to disease. *Cell Calcium*. 2021;94:102356. doi: 10.1016/j.ceca.2021.102356
20. Ozaki T, Tomita H, Tamai M, Ishiguro S. Characteristics of mitochondrial calpains. *J Biochem*. 2007;142:365–376. doi: 10.1093/jb/mvm143
21. Chen Q, Paillard M, Gomez L, Ross T, Hu Y, Xu A, Lesnefsky EJ. Activation of mitochondrial μ-calpain increases AIF cleavage in cardiac mitochondria during ischemia-reperfusion. *Biochem Biophys Res Commun*. 2011;415:533–538. doi: 10.1016/j.bbrc.2011.10.037
22. Chen Q, Thompson J, Hu Y, Dean J, Lesnefsky EJ. Inhibition of the ubiquitous calpains protects complex I activity and enables improved mitophagy in the heart following ischemia-reperfusion. *Am J Physiol Cell Physiol*. 2019;317:C910–C921. doi: 10.1152/ajpcell.00190.2019
23. Chen Q, Thompson J, Hu Y, Lesnefsky EJ. Reversing mitochondrial defects in aged hearts: role of mitochondrial calpain activation. *Am J Physiol Cell Physiol*. 2022;322:C296–C310. doi: 10.1152/ajpcell.00279.2021
24. Potz BA, Sabe SA, Scrimgeour LA, Sabe AA, Harris DD, Abid MR, Clements RT, Sellke FW. Calpain inhibition decreases oxidative stress via mitochondrial regulation in a swine model of chronic myocardial ischemia. *Free Radic Biol Med*. 2023;208:700–707. doi: 10.1016/j.freeradbiomed.2023.09.028
25. Chelko SP, Keceli G, Carpi A, Doti N, Agrimi J, Asimaki A, Beti CB, Miyamoto M, Amat-Codina N, Bedja D, et al. Exercise triggers CAPN1-mediated AIF truncation, inducing myocyte cell death in arrhythmogenic cardiomyopathy. *Sci Transl Med*. 2021;13:eabf0891. doi: 10.1126/scitranslmed.abf0891
26. Chen L, Gong Q, Stice JP, Knowlton AA. Mitochondrial OPA1, apoptosis, and heart failure. *Cardiovasc Res*. 2009;84:91–99. doi: 10.1093/cvr/cvp181
27. Luongo TS, Lambert JP, Yuan A, Zhang X, Gross P, Song J, Shanmughapriya S, Gao E, Jain M, Houser SR, et al. The mitochondrial calcium uniporter matches energetic supply with cardiac workload during stress and modulates permeability transition. *Cell Rep*. 2015;12:23–34. doi: 10.1016/j.celrep.2015.06.017
28. Sikkel MB, Francis DP, Howard J, Gordon F, Rowlands C, Peters NS, Lyon AR, Harding SE, MacLeod KT. Hierarchical statistical techniques are necessary to draw reliable conclusions from analysis of isolated cardiomyocyte studies. *Cardiovasc Res*. 2017;113:1743–1752. doi: 10.1093/cvr/cvx151
29. Suetomi T, Yano M, Uchinoumi H, Fukuda M, Hino A, Ono M, Xu X, Tateishi H, Okuda S, Doi M, et al. Mutation-linked defective interdomain interactions within ryanodine receptor cause aberrant Ca^{2+}release leading to catecholaminergic polymorphic ventricular tachycardia. *Circulation*. 2011;124:682–694. doi: 10.1161/CIRCULATIONAHA.111.023259
30. Tester DJ, Spoon DB, Valdivia HH, Makielski JC, Ackerman MJ. Targeted mutational analysis of the RyR2-encoded cardiac ryanodine receptor in sudden unexplained death: a molecular autopsy of 49 medical examiner/coroner's cases. *Mayo Clin Proc*. 2004;79:1380–1384. doi: 10.4065/79.11.1380
31. Priori SG, Napolitano C, Tiso N, Memmi M, Vignati G, Bloise R, Sorrentino V, Danieli GA. Mutations in the cardiac ryanodine receptor gene (hRyR2) underlie catecholaminergic polymorphic ventricular tachycardia. *Circulation*. 2001;103:196–200. doi: 10.1161/01.cir.103.2.196
32. George CH, Higgs GV, Lai FA. Ryanodine receptor mutations associated with stress-induced ventricular tachycardia mediate increased calcium release in stimulated cardiomyocytes. *Circ Res*. 2003;93:531–540. doi: 10.1161/01.RES.0000091335.07574.86
33. Swan H, Piippo K, Viitasalo M, Heikkilä P, Paavonen T, Kainulainen K, Kere J, Keto P, Kontula K, Toivonen L. Arrhythmic disorder mapped to chromosome 1q42-q43 causes malignant polymorphic ventricular tachycardia in structurally normal hearts. *J Am Coll Cardiol*. 1999;34:2035–2042. doi: 10.1016/s0735-1097(99)00461-1
34. Leenhardt A, Lucet V, Denjoy I, Grau F, Ngoc DD, Coumel P. Catecholaminergic polymorphic ventricular tachycardia in children. A 7-year follow-up of 21 patients. *Circulation*. 1995;91:1512–1519. doi: 10.1161/01.cir.91.5.1512
35. Suzuki J, Kanemaru K, Ishii K, Ohkura M, Okubo Y, Iino M. Imaging intraorganellar Ca2+ at subcellular resolution using CEPIA. *Nat Commun*. 2014;5:4153. doi: 10.1038/ncomms5153
36. Pak VV, Ezerina D, Lyublinskaya OG, Pedre B, Tyurin-Kuzmin PA, Mishina NM, Thauvin M, Young D, Wahni K, Martínez Gache SA, et al. Ultrasensitive genetically encoded indicator for hydrogen peroxide identifies roles for the oxidant in cell migration and mitochondrial function. *Cell Metab*. 2020;31:642–653.e6. doi: 10.1016/j.cmet.2020.02.003
37. Akerboom J, Carreras Calderón N, Tian L, Wabnig S, Prigge M, Tolö J, Gordus A, Orger MB, Severi KE, Macklin JJ, et al. Genetically encoded calcium indicators for multi-color neural activity imaging and combination with optogenetics. *Front Mol Neurosci*. 2013;6:2. doi: 10.3389/fnmol.2013.00002
38. Raffaello A, De Stefani D, Sabbadin D, Teardo E, Merli G, Picard A, Checchetto V, Moro S, Szabò I, Rizzuto R. The mitochondrial calcium uniporter is a multimer that can include a dominant-negative pore-forming subunit. *EMBO J*. 2013;32:2362–2376. doi: 10.1038/emboj.2013.157
39. Plovanich M, Bogorad RL, Sancak Y, Kamer KJ, Strittmatter L, Li AA, Girgis HS, Kuchimanchi S, De Groot J, Speciner L, et al. MICU2, a paralog of MICU1, resides within the mitochondrial uniporter complex to regulate calcium handling. *PLoS One*. 2013;8:e55785. doi: 10.1371/journal.pone.0055785
40. Paillard M, Huang KT, Weaver D, Lambert JP, Elrod JW, Hajnóczky G. Altered composition of the mitochondrial Ca^{2+}uniporter in the failing human heart. *Cell Calcium*. 2022;105:102618. doi: 10.1016/j.ceca.2022.102618
41. Maack C, Cortassa S, Aon MA, Ganesan AN, Liu T, O'Rourke B. Elevated cytosolic Na+ decreases mitochondrial Ca2+ uptake during excitation-contraction coupling and impairs energetic adaptation in cardiac myocytes. *Circ Res*. 2006;99:172–182. doi: 10.1161/01.RES.0000232546.92777.05
42. Zhao Y, Araki S, Wu J, Teramoto T, Chang YF, Nakano M, Abdelfattah AS, Fujiwara M, Ishihara T, Nagai T, et al. An expanded palette of genetically encoded Ca^{2+} indicators. *Science*. 2011;333:1888–1891. doi: 10.1126/science.1208592
43. Waldeck-Weiermair M, Gottschalk B, Madreiter-Sokolowski CT, Ramadani-Muja J, Ziomek G, Klec C, Burgstaller S, Bischof H, Depaoli MR, Eroglu E, et al. Development and application of sub-mitochondrial targeted Ca^{2+} biosensors. *Front Cell Neurosci*. 2019;13:449. doi: 10.3389/fncel.2019.00449
44. Lam SS, Martell JD, Kamer KJ, Deerinck TJ, Ellisman MH, Mootha VK, Ting AY. Directed evolution of APEX2 for electron microscopy and proximity labeling. *Nat Methods*. 2015;12:51–54. doi: 10.1038/nmeth.3179
45. Croall DE, DeMartino GN. Calcium-activated neutral protease (calpain) system: structure, function, and regulation. *Physiol Rev*. 1991;71:813–847. doi: 10.1152/physrev.1991.71.3.813
46. Ono Y, Sorimachi H. Calpains: an elaborate proteolytic system. *Biochim Biophys Acta*. 2012;1824:224–236. doi: 10.1016/j.bbapap.2011.08.005
47. Murphy RM, Dutka TL, Horvath D, Bell JR, Delbridge LM, Lamb GD. Ca2+-dependent proteolysis of junctophilin-1 and junctophilin-2 in skeletal and cardiac muscle. *J Physiol*. 2013;591:719–729. doi: 10.1113/jphysiol.2012.243279
48. Wu CY, Chen B, Jiang YP, Jia Z, Martin DW, Liu S, Entcheva E, Song LS, Lin RZ. Calpain-dependent cleavage of junctophilin-2 and T-tubule remodeling in a mouse model of reversible heart failure. *J Am Heart Assoc*. 2014;3:e000527. doi: 10.1161/JAHA.113.000527
49. Varanita T, Soriano ME, Romanello V, Zaglia T, Quintana-Cabrera R, Semenzato M, Menabò R, Costa V, Civiletto G, Pesce P, et al. The OPA1-dependent mitochondrial cristae remodeling pathway controls atrophic, apoptotic, and ischemic tissue damage. *Cell Metab*. 2015;21:834–844. doi: 10.1016/j.cmet.2015.05.007
50. Wang J, Ciampa G, Zheng D, Shi Q, Chen B, Abel ED, Peng T, Hall DD, Song LS. Calpain-2 specifically cleaves Junctophilin-2 at the same site as calpain-1 but with less efficacy. *Biochem J*. 2021;478:3539–3553. doi: 10.1042/BCJ20210629

51. Chaban Y, Boekema EJ, Dudkina NV. Structures of mitochondrial oxidative phosphorylation supercomplexes and mechanisms for their stabilization. *Biochim Biophys Acta*. 2014;1837:418–426. doi: 10.1016/j.bbabio.2013.10.004
52. Clements RT, Terentyeva R, Hamilton S, Janssen PML, Roder K, Martin BY, Perger F, Schneider T, Nichtova Z, Das AS, et al. Sexual dimorphism in bidirectional SR-mitochondria crosstalk in ventricular cardiomyocytes. *Basic Res Cardiol*. 2023;118:15. doi: 10.1007/s00395-023-00988-1
53. Cogliati S, Frezza C, Soriano ME, Varanita T, Quintana-Cabrera R, Corrado M, Cipolat S, Costa V, Casarin A, Gomes LC, et al. Mitochondrial cristae shape determines respiratory chain supercomplexes assembly and respiratory efficiency. *Cell*. 2013;155:160–171. doi: 10.1016/j.cell.2013.08.032
54. Veress R, Terentyeva R, Belevych AE, Perger F, Nichtova Z, Pokrass A, Cheng Y, Chorna S, Deschenes I, Gyorke S, et al. Pharmacological enhancement of small conductance Ca^{2+}-activated K^+ channels suppresses cardiac arrhythmias in a mouse model of catecholaminergic polymorphic ventricular tachycardia. *Circ Res*. 2025;137:386–399. doi: 10.1161/CIRCRESAHA.124.325477
55. Szulik MW, Valdez S, Walsh M, Davis K, Bia R, Horiuchi E, O'Very S, Laxman AK, Sandaklie-Nicolova L, Eberhardt DR, et al. SMYD1a protects the heart from ischemic injury by regulating OPA1-mediated cristae remodeling and supercomplex formation. *Basic Res Cardiol*. 2023;118:20. doi: 10.1007/s00395-023-00991-6
56. Wang Y, Chen B, Huang CK, Guo A, Wu J, Zhang X, Chen R, Chen C, Kutschke W, Weiss RM, et al. Targeting calpain for heart failure therapy: implications from multiple murine models. *JACC Basic Transl Sci*. 2018;3:503–517. doi: 10.1016/j.jacbts.2018.05.004
57. Croall DE, Ersfeld K. The calpains: modular designs and functional diversity. *Genome Biol*. 2007;8:218. doi: 10.1186/gb-2007-8-6-218
58. Hamilton S, Polina I, Terentyeva R, Bronk P, Kim TY, Roder K, Clements RT, Koren G, Choi BR, Terentyev D. PKA phosphorylation underlies functional recruitment of sarcolemmal SK2 channels in ventricular myocytes from hypertrophic hearts. *J Physiol*. 2020;598:2847–2873. doi: 10.1113/JP277618
59. Dries E, Santiago DJ, Gilbert G, Lenaerts I, Vandenberk B, Nagaraju CK, Johnson DM, Holemans P, Roderick HL, Macquaide N, et al. Hyperactive ryanodine receptors in human heart failure and ischaemic cardiomyopathy reside outside of couplons. *Cardiovasc Res*. 2018;114:1512–1524. doi: 10.1093/cvr/cvy088
60. Kim TY, Terentyeva R, Roder KH, Li W, Liu M, Greener I, Hamilton S, Polina I, Murphy KR, Clements RT, et al. SK channel enhancers attenuate Ca2+-dependent arrhythmia in hypertrophic hearts by regulating mito-ROS-dependent oxidation and activity of RyR. *Cardiovasc Res*. 2017;113:343–353. doi: 10.1093/cvr/cvx005
61. Kohlhaas M, Liu T, Knopp A, Zeller T, Ong MF, Böhm M, O'Rourke B, Maack C. Elevated cytosolic Na+ increases mitochondrial formation of reactive oxygen species in failing cardiac myocytes. *Circulation*. 2010;121:1606–1613. doi: 10.1161/CIRCULATIONAHA.109.914911
62. Liu H, Zhao Y, Xie A, Kim TY, Terentyeva R, Liu M, Shi G, Feng F, Choi BR, Terentyev D, et al. Interleukin-1β, oxidative stress, and abnormal calcium handling mediate diabetic arrhythmic risk. *JACC Basic Transl Sci*. 2021;6:42–52. doi: 10.1016/j.jacbts.2020.11.002
63. Terentyev D, Györke I, Belevych AE, Terentyeva R, Sridhar A, Nishijima Y, de Blanco EC, Khanna S, Sen CK, Cardounel AJ, et al. Redox modification of ryanodine receptors contributes to sarcoplasmic reticulum Ca2+ leak in chronic heart failure. *Circ Res*. 2008;103:1466–1472. doi: 10.1161/CIRCRESAHA.108.184457
64. Nikolaienko R, Bovo E, Kahn D, Gracia R, Jamrozik T, Zima AV. Cysteines 1078 and 2991 cross-linking plays a critical role in redox regulation of cardiac ryanodine receptor (RyR). *Nat Commun*. 2023;14:4498. doi: 10.1038/s41467-023-40268-z
65. Zima AV, Blatter LA. Redox regulation of cardiac calcium channels and transporters. *Cardiovasc Res*. 2006;71:310–321. doi: 10.1016/j.cardiores.2006.02.019
66. Erickson JR, Joiner ML, Guan X, Kutschke W, Yang J, Oddis CV, Bartlett RK, Lowe JS, O'Donnell SE, Aykin-Burns N, et al. A dynamic pathway for calcium-independent activation of CaMKII by methionine oxidation. *Cell*. 2008;133:462–474. doi: 10.1016/j.cell.2008.02.048
67. Luczak ED, Anderson ME. CaMKII oxidative activation and the pathogenesis of cardiac disease. *J Mol Cell Cardiol*. 2014;73:112–116. doi: 10.1016/j.yjmcc.2014.02.004
68. Mattiazzi A, Bassani RA, Escobar AL, Palomeque J, Valverde CA, Vila Petroff M, Bers DM. Chasing cardiac physiology and pathology down the CaMKII cascade. *Am J Physiol Heart Circ Physiol*. 2015;308:H1177–H1191. doi: 10.1152/ajpheart.00007.2015
69. Hamilton S, Terentyeva R, Bogdanov V, Kim TY, Perger F, Yan J, Ai X, Carnes CA, Belevych AE, George CH, et al. Ero1α-dependent Erp44 dissociation from RyR2 contributes to cardiac arrhythmia. *Circ Res*. 2022;130:711–724. doi: 10.1161/CIRCRESAHA.121.320531
70. Gonano LA, Sepúlveda M, Morell M, Toteff T, Racioppi MF, Lascano E, Negroni J, Fernández Ruocco MJ, Medei E, Neiman G, et al. Non-β-blocking carvedilol analog, VK-II-86, prevents ouabain-induced cardiotoxicity. *Circ J*. 2018;83:41–51. doi: 10.1253/circj.CJ-18-0247
71. Maack C, O'Rourke B. Excitation-contraction coupling and mitochondrial energetics. *Basic Res Cardiol*. 2007;102:369–392. doi: 10.1007/s00395-007-0666-z
72. Balaban RS. The role of Ca(2+) signaling in the coordination of mitochondrial ATP production with cardiac work. *Biochim Biophys Acta*. 2009;1787:1334–1341. doi: 10.1016/j.bbabio.2009.05.011
73. Tow BD, Deb A, Neupane S, Patel SM, Reed M, Loper AB, Eliseev RA, Knollmann BC, Györke S, Liu B. SR-mitochondria crosstalk shapes Ca signalling to impact pathophenotype in disease models marked by dysregulated intracellular Ca release. *Cardiovasc Res*. 2022;118:2819–2832. doi: 10.1093/cvr/cvab324
74. Schweitzer MK, Wilting F, Sedej S, Dreizehnter L, Dupper NJ, Tian Q, Moretti A, My I, Kwon O, Priori SG, et al. Suppression of arrhythmia by enhancing mitochondrial Ca^{2+} uptake in catecholaminergic ventricular tachycardia models. *JACC Basic Transl Sci*. 2017;2:737–747. doi: 10.1016/j.jacbts.2017.06.008
75. Velmurugan S, Liu T, Chen KC, Despa F, O'Rourke B, Despa S. Distinct effects of mitochondrial Na^+/Ca^{2+} exchanger inhibition and Ca^{2+} uniporter activation on Ca^{2+} sparks and arrhythmogenesis in diabetic rats. *J Am Heart Assoc*. 2023;12:e029997. doi: 10.1161/JAHA.123.029997
76. Kwong JQ, Lu X, Correll RN, Schwanekamp JA, Vagnozzi RJ, Sargent MA, York AJ, Zhang J, Bers DM, Molkentin JD. The mitochondrial calcium uniporter selectively matches metabolic output to acute contractile stress in the heart. *Cell Rep*. 2015;12:15–22. doi: 10.1016/j.celrep.2015.06.002
77. Wu Y, Rasmussen TP, Koval OM, Joiner ML, Hall DD, Chen B, Luczak ED, Wang Q, Rokita AG, Wehrens XH, et al. The mitochondrial uniporter controls fight or flight heart rate increases. *Nat Commun*. 2015;6:6081. doi: 10.1038/ncomms7081. Erratum in: *Nat Commun*. 2015;6:7241
78. Xie A, Song Z, Liu H, Zhou A, Shi G, Wang Q, Gu L, Liu M, Xie LH, Qu Z, et al. Mitochondrial Ca^{2+} influx contributes to arrhythmic risk in nonischemic cardiomyopathy. *J Am Heart Assoc*. 2018;7:e007805. doi: 10.1161/JAHA.117.007805
79. Bertero E, Maack C. Calcium signaling and reactive oxygen species in mitochondria. *Circ Res*. 2018;122:1460–1478. doi: 10.1161/CIRCRESAHA.118.310082
80. Cogliati S, Calvo E, Loureiro M, Guaras AM, Nieto-Arellano R, Garcia-Poyatos C, Ezkurdia I, Mercader N, Vazquez J, Enriquez JA. Mechanism of super-assembly of respiratory complexes III and IV. *Nature*. 2016;539:579–582. doi: 10.1038/nature20157
81. Baker N, Patel J, Khacho M. Linking mitochondrial dynamics, cristae remodeling and supercomplex formation: how mitochondrial structure can regulate bioenergetics. *Mitochondrion*. 2019;49:259–268. doi: 10.1016/j.mito.2019.06.003
82. Watson LE, Sheth M, Denyer RF, Dostal DE. Baseline echocardiographic values for adult male rats. *J Am Soc Echocardiogr*. 2004;17:161–167. doi: 10.1016/j.echo.2003.10.010
83. Williams GS, Boyman L, Lederer WJ. Mitochondrial calcium and the regulation of metabolism in the heart. *J Mol Cell Cardiol*. 2015;78:35–45. doi: 10.1016/j.yjmcc.2014.10.019
84. Báthori G, Csordás G, Garcia-Perez C, Davies E, Hajnóczky G. Ca2+-dependent control of the permeability properties of the mitochondrial outer membrane and voltage-dependent anion-selective channel (VDAC). *J Biol Chem*. 2006;281:17347–17358. doi: 10.1074/jbc.M600906200
85. Terentyev D, Rees CM, Li W, Cooper LL, Jindal HK, Peng X, Lu Y, Terentyeva R, Odening KE, Daley J, et al. Hyperphosphorylation of RyRs underlies triggered activity in transgenic rabbit model of LQT2 syndrome. *Circ Res*. 2014;115:919–928. doi: 10.1161/CIRCRESAHA.115.305146
86. Kirichok Y, Krapivinsky G, Clapham DE. The mitochondrial calcium uniporter is a highly selective ion channel. *Nature*. 2004;427:360–364. doi: 10.1038/nature02246
87. Zhou Z, Matlib MA, Bers DM. Cytosolic and mitochondrial Ca2+ signals in patch clamped mammalian ventricular myocytes. *J Physiol*. 1998;507(Pt 2):379–403. doi: 10.1111/j.1469-7793.1998.379bt.x
88. Tomar D, Thomas M, Garbincius JF, Kolmetzky DW, Salik O, Jadiya P, Joseph SK, Carpenter AC, Hajnóczky G, Elrod JW. MICU1 regulates mitochondrial cristae structure and function independently of the

mitochondrial Ca^{2+}uniporter channel. *Sci Signal*. 2023;16:eabi8948. doi: 10.1126/scisignal.abi8948
89. Zheng D, Cao T, Zhang LL, Fan GC, Qiu J, Peng TQ. Targeted inhibition of calpain in mitochondria alleviates oxidative stress-induced myocardial injury. *Acta Pharmacol Sin*. 2021;42:909–920. doi: 10.1038/s41401-020-00526-y
90. Mohsin AA, Thompson J, Hu Y, Hollander J, Lesnefsky EJ, Chen Q. Endoplasmic reticulum stress-induced complex I defect: central role of calcium overload. *Arch Biochem Biophys*. 2020;683:108299. doi: 10.1016/j.abb.2020.108299
91. Concordet JP, Haeussler M. CRISPOR: intuitive guide selection for CRISPR/Cas9 genome editing experiments and screens. *Nucleic Acids Res*. 2018;46:W242–W245. doi: 10.1093/nar/gky354
92. Perez AR, Pritykin Y, Vidigal JA, Chhangawala S, Zamparo L, Leslie CS, Ventura A. GuideScan software for improved single and paired CRISPR guide RNA design. *Nat Biotechnol*. 2017;35:347–349. doi: 10.1038/nbt.3804
93. Tycko J, Wainberg M, Marinov GK, Ursu O, Hess GT, Ego BK, Aradhana, Li A, Truong A, Trevino AE, et al. Mitigation of off-target toxicity in CRISPR-Cas9 screens for essential non-coding elements. *Nat Commun*. 2019;10:4063. doi: 10.1038/s41467-019-11955-7
94. McBurney MW, Fournier S, Schmidt-Kastner PK, Jardine K, Craig J. Unstable integration of transfected DNAs into embryonal carcinoma cells. *Somat Cell Mol Genet*. 1994;20:529–540. doi: 10.1007/BF02255843
95. Khalifa AR, Abdel-Rahman EA, Mahmoud AM, Ali MH, Noureldin M, Saber SH, Mohsen M, Ali SS. Sex-specific differences in mitochondria biogenesis, morphology, respiratory function, and ROS homeostasis in young mouse heart and brain. *Physiol Rep*. 2017;5:e13125. doi: 10.14814/phy2.13125